LEONARDO ARAUJO

HISTOPATHOLOGY OF MANGO - *Ceratocystis fimbriata* INTERACTION

Tese apresentada à Universidade Federal de Viçosa, como parte das exigências do Programa de Pós-Graduação em Fitopatologia, para obtenção do título de *Doctor Scientiae*.

VIÇOSA
MINAS GERAIS – BRASIL
2014

Ficha catalográfica preparada pela Seção de Catalogação e Classificação da Biblioteca Central da UFV

T
A663h
2014

Araujo, Leonardo, 2014-
Histopathology of mango - *Ceratocystis fimbriata* interaction / Leonardo Araujo. – Viçosa, MG, 2014.
x, 85 f. : il. (algumas color.) ; 29 cm.

Texto em inglês e português.
Orientador: Fabrício de Ávila Rodrigues.
Tese (doutorado) - Universidade Federal de Viçosa.
Inclui bibliografia.

1. Seca-da-mangueira. 2. Manga - Doenças e pragas - Controle. 3. Fenóis. I. Universidade Federal de Viçosa. Departamento de Fitopatologia. Programa de Pós-Graduação em Fitopatologia. II. Título.

CDD 22. ed. 632.465

LEONARDO ARAUJO

HISTOPATHOLOGY OF MANGO - *Ceratocystis fimbriata* INTERACTION

Tese apresentada à Universidade Federal de Viçosa, como parte das exigências do Programa de Pós-Graduação em Fitopatologia, para obtenção do título de *Doctor Scientiae*.

APROVADA: em 28 de janeiro de 2014

Prof. Acelino Couto Alfenas

Prof. Eduardo Alves

Prof. Luis Cláudio Vieira da Cunha

Dra. Maria Fernanda Antunes da Cruz

Prof. Fabrício Ávila Rodrigues

Orientador

Aos meus amados pais Elizabete M. Araujo e
Valmir D. Araujo, à minha esposa Kamila,
e à minha filha Ana Beatriz

OFEREÇO e DEDICO

AGRADECIMENTOS

À Deus.

À Universidade Federal de Viçosa, ao Departamento de Fitopatologia e ao Programa de Pós-graduação em Fitopatologia, por proporcionarem condições de realizar este trabalho.

Ao Núcleo de Microscopia e Microanálise da Universidade Federal de Viçosa pelo uso dos equipamentos.

Ao Conselho Nacional de Desenvolvimento Científico e Tecnológico (CNPq) pelo apoio financeiro.

A Vale S.A., pelo apoio financeiro para realização dos experimentos.

Aos representantes da Vale S.A., Camila Meireles, Domenica Blundi, Sandoval Carneiro pelo suporte técnico.

Aos funcionários do Departamento de Fitopatologia e Setor do Viveiro do Café, especialmente ao Senhor Mário e sua família, pela amizade e pelo apoio técnico.

Ao Professor Acelino Couto Alfenas e ao colega Leonardo Sarno Soares Oliveira por gentilmente terem fornecido os isolados de *C. fimbriata* utilizados neste estudo.

Aos professores do Departamento de Fitopatologia da Universidade Federal de Viçosa, pelos ensinamentos.

Ao professor Marciel João Stadnik por todo ensinamento e grandes conselhos dados que me ajudaram muito durante minha vida acadêmica.

Ao Professor Fabrício Ávila Rodrigues pela orientação pelo apoio, pela amizade e por seu exemplo de disciplina, competência e profissionalismo.

Aos meus pais, Elizabete e Valmir, meu padrinho Vilson, minha avó Egídia, minha esposa Kamila e minha filha Ana Beatriz pelo amor, pelo carinho, pela ajuda, pelo apoio incondicional e pelo referencial de dedicação e honestidade.

Aos integrantes do Laboratório de Interação Planta-Patógeno, André, Alessandro, Carlos, Daniel, Leandro, Maria, Patrícia, Renata, Sandro e Vinicíus pelo apoio e pela amizade e em especial para Isaías, Jonas, Maria Fernanda, Wiler e Wilka que além do companheirismo contribuíram diretamente para a realização deste trabalho.

A todos que direta ou indiretamente contribuíram para a realização deste trabalho.

MUITO OBRIGADO!!!

BIOGRAFIA

LEONARDO ARAUJO, filho de Elizabete Martins Araujo e Valmir Domingos Araujo, nasceu em 02 de outubro de 1982, em Florianópolis, Estado de Santa Catarina. Ingressou em 2002, no curso de Agronomia da Universidade Federal de Santa Catarina (UFSC), Florianópolis-SC, concluindo-o em agosto de 2007. Em março de 2008, iniciou o curso de Mestrado do Programa de Pós-Graduação em Recursos Genéticos Vegetais da Universidade Federal de Santa Catarina (UFSC), Florianópolis-SC, concluindo-o em fevereiro de 2010. Em agosto de 2010, ingressou no curso de Doutorado do Programa de Pós-Graduação em Fitopatologia na Universidade Federal de Viçosa (UFV), Viçosa-MG, submetendo-se à defesa em 28 de janeiro de 2014.

SUMÁRIO

RESUMO

ARAUJO, Leonardo, D. Sc., Universidade Federal de Viçosa, Janeiro de 2014. **Hitopatologia da interação mangueira - *Ceratocystis fimbriata***. Orientador: Fabrício Ávila Rodrigues. Coorientador: Gleiber Quintão Furtado.

A murcha de Ceratocystis, causada por *Ceratocystis fimbriata*, é uma das doenças mais importantes que afetam a produção de manga no Brasil. Informações sobre o processo de infecção de *C. fimbriata* nos tecidos do caule de diferentes cultivares de mangueira e os mecanismos de resistência do hospedeiro contra a infecção do patógeno é pouco disponível na literatura. Assim, o objetivo geral deste trabalho foi investigar por meio de cortes histopatológicos possíveis mecanismos de defesa de diferentes cultivares de mangueira formados após a infecção de *C. fimbriata*. No primeiro estudo, investigou-se histopatologicamente o processo de infecção de dois isolados de *C. fimbriata* (CEBS15 e MSAK16) em cinco cultivares de mangueira e para isso secções de caule, obtidas no ponto de inoculação foram preparadas para observações histopatológicas em microscopia de luz. Os fatores cultivares de manga e isolados de *C. fimbriata* e suas interações foram significativos para todas as medidas de desenvolvimento da doença. Plantas das cultivares Espada, Haden e Palmer inoculadas com os dois isolados de *C. fimbriata* foram mais suscetíveis, enquanto que plantas das cultivares Tommy Atkins e Ubá foram moderadamente resistentes e resistentes, respectivamente. Histopatologicamente os isolados fúngicos colonizavam intensamente os tecidos do caule de plantas das cultivares suscetíveis Espada, Haden e Palmer, a partir do colênquima e se moviam na direção ao parênquima cortical, aos vasos do xilema e ao parênquima medular. De modo contrário, nos tecidos do caule de plantas das cultivares resistentes Tommy Atkins e Ubá, muitas células reagiram à infecção de *C. fimbriata* pela acumulação de material amorfo que contribuiu para que muitas hifas fúngicas aparecerem mortas. Os resultados do presente estudo indicam a importância dos compostos fenólicos para resistência de cultivares de manga contra a infecção de *C. fimbriata*. No segundo estudo determinou-se a resposta de duas cultivares de manga, Ubá (resistente) e Haden (suscetível), à infecção por um isolado de *C. fimbriata* (MSAK16), examinando a ocorrência de zonas de barreira e a acumulação de elementos minerais e compostos fenólicos. Avaliou-se o progresso da doença nos tecidos do caule e as respostas histopatológicas de plantas inoculadas das cultivares Haden e Ubá. Secções

do caule obtidas a partir dos pontos de inoculação foram utilizadas para observação por microscopia de fluorescência, microscopia eletrônica de varredura (MEV) associada à microanálise de raios-X e microscopia eletrônica de transmissão (TEM). Com base na evolução da doença a Haden foi mais suscetível à murcha do Ceratocystis, comparado a Ubá. Tecidos adjacentes às áreas necróticas das secções de caule da Ubá apresentavam maior autofluorescência que da Haden. De acordo com a microanálise de raio-X, os picos e as deposições de enxofre (S) e cálcio (Ca) nos tecidos do caule da Ubá foram maiores que da Haden. Observações em MEV permitiram evidenciar abundantes hifas fúngicas, clamidósporos e estruturas semelhantes a peritécio de *C. fimbriata* nos tecidos da Haden. Em contraste, as estruturas de *C. fimbriata* foram pouco observadas no tecido do caule da Ubá. Observações de TEM mostraram que hifas longas e grossas de *C. fimbriata* colonizavam as células de fibras e parênquima, bem como os vasos do xilema dos tecidos de caule da Haden. Ao contrário na Ubá as hifas fúngicas eram delgadas e muitas vezes cercadas ou presas por material amorfo eletro denso, com muitas hifas com aparência de morta. As paredes das células do parênquima da Haden foram completamente degradadas pela colonização de *C. fimbriata*, enquanto que as paredes das células do parênquima da Ubá raramente mostraram sinais de degradação, principalmente porque elas foram protegidas pelo acúmulo de material amorfo. Na Haden, hifas penetraram na membrana da pontuação, alcançando os vasos do xilema dos tecidos de caule sem impedimento aparente, enquanto que nos tecidos do caule da Uba, a penetração das hifas foi frequentemente impedida pela presença de material amorfo. Os resultados do presente estudo sugerem que as zonas da barreira associadas com depósitos de S e Ca, e à acumulação de compostos fenólicos desempenham um papel essencial na resistência da mangueira contra a infecção de *C. fimbriata*.

ABSTRACT

ARAUJO, Leonardo, D. Sc., Universidade Federal de Viçosa, January, 2014. **Histopathology of mango - *Ceratocystis fimbriata* interaction**. Adviser: Fabrício Ávila Rodrigues. Co-adviser: Gleiber Quintão Furtado.

Mango wilt, caused by *Ceratocystis fimbriata*, is one of the most important diseases affecting mango yields in Brazil. Information regarding the infection process of *C. fimbriata* in the stem tissues of mango from different cultivars and the mechanisms of host resistance against pathogen infection is scarcely available in the literature. Thus, the general objective of this work was investigate through cuts histopathological possible defense mechanisms of different cultivars of mango plants formed after infection of *C. fimbriata*. In the first study, was investigated histopathologically how the infection process of two isolates of *C. fimbriata* (CEBS15 and MSAK16) in five mango plants cultivars and for it stem sections were obtained in the inoculation and prepared for histopathological observations in light microscopy. The factors mango cultivars and *C. fimbriata* isolates and their interaction were significant for all measures of disease development. Plants from the cultivars Espada, Haden and Palmer inoculated with two isolates of *C. fimbriata* were more susceptible, whereas plants from the cultivars Tommy and Ubá were moderately resistant and resistant, respectively. Histopathologically, fungal isolates intensively colonized the stem tissues of plants from the susceptible cultivars Espada, Haden and Palmer, starting from the collenchyma and moving in the direction of the cortical parenchyma, xylem vessels and pith parenchyma. By contrast, on the stem tissues of plants from the resistant cultivars Tommy Atkins and Ubá, most of the cells reacted to *C. fimbriata* infection by accumulating amorphous material which contributed to many fungal hyphae appearing dead. The results from the present study indicated the importance of phenolic-like compounds for resistance of mango plants cultivars against the infection of *C. fimbriata*. In the second study was determined the response of two mango cultivars, Ubá (resistant) and Haden (susceptible), to infection by one isolate of *C. fimbriata* (MSAK16) by examining the occurrence of barrier zones and the accumulation of mineral elements and phenolic-like compounds. It was evaluated the disease progress in the tissues of the stem and histopathological response of plants inoculated cultivars Haden and Uba. Stem sections obtained at the inoculation points were used for observation by fluorescence

microscopy, scanning electron microscopy (SEM) associated with X-ray microanalysis and transmission electron microscopy (TEM). Based on disease progress, the Haden was more susceptible to mango wilt than Ubá. Tissue proximal to the necrotic areas on the stem sections from Ubá showed stronger autofluorescence compared with Haden. According to X-ray microanalysis, the peaks and depositions of sulfur (S) and calcium (Ca) on the stem tissue from Ubá were greater than for Haden. SEM observations, allowed note abundant fungal hyphae, chlamydospores and perithecia-like structures of *C. fimbriata* in the stem tissue from Haden. In contrast, the structures of *C. fimbriata* were barely observed in the stem tissue from Ubá. TEM observations showed that long and thickened hyphae of *C. fimbriata* colonized in the fiber and parenchyma cells as well as on the xylem vessels of the stem tissue from Haden. In contrast, from Ubá the fungal hyphae were thin, faint and often surrounded or trapped by dense amorphous material, with most hyphae with the appearance of dead. The parenchyma cell walls from Haden were completely degraded due to the colonization by *C. fimbriata*, while the parenchyma cell walls from Ubá rarely showed signs of degradation, primarily because they were protected by the accumulation of amorphous material. In Haden, fungal hyphae penetrated the pit membrane, reaching the xylem vessels of the stem tissue without apparently impediment, whereas on the stem tissue from Ubá, the penetration of fungal hyphae was often impeded by the presence of amorphous material. The results from the present study suggest that the barrier zones associated with deposits of S and Ca and the accumulation of phenolic-like compounds play a pivotal role in the resistance of mango plants against infection by *C. fimbriata.*

GENERAL INTRODUCTION

Mango (*Mangifera indica* L.) is one of the most important tropical fruit worldwide. Asia and the Pacific region are the major mango producers, followed by Latin America, the Caribbean and Africa (Food and Agriculture Organization of the United Nations; FAO, 2013). Brazil is the seventh largest mango producer in the world (FAO, 2013) and the cultivars Espada, Haden, Palmer and Tommy Atkins are the most important for fresh consumption, whereas cultivar Ubá has been used for juice production (Carvalho *et al.*, 2004; Ribeiro *et al.*, 2008).

The adaptability of mango cultivars to different environmental conditions and their resistance to multiple diseases are among the factors that greatly improve yield (Carvalho *et al.*, 2004). Although it is presently not quantified it is believed that mango wilt, caused by *Ceratocystis fimbriata* Ellis & Halst. affect mango production (Viegas, 1960; Ferreira *et al.*, 2010). *C. fimbriata* causes the death of the entire tree either a few months after the fungus penetrates the roots or more slowly if the infection takes place on wounded branches of the canopy (Viegas, 1960; Ribeiro, 2005). Typical symptoms of mango wilt are wilting and browning of the leaves on single branches and gum exudation from the trunks (Viegas, 1960; Ribeiro, 2005). As the infection of *C. fimbriata* progresses, the internal and external stem tissue becomes dark brown due to intensive necrosis (Viegas, 1960; Ribeiro, 2005).

The fungus *C. fimbriat*a have been introduced into many regions of the world by propagative materials from introductions by humans (CAB International, 2005). Agricultural practices such as pruning wounds are common entry points for *C. fimbriata* and often those are made by contaminated cutting tools (Viégas, 1960; CAB International, 2005). However, the fungus is soilborne, and root infections are common by chlamydospores (aleurioconidia) that have thick-walled and facilitates the survival in soil (CAB International, 2005; Ribeiro, 2005). Furthermore, many *Ceratocystis* spp. produce fruiting bodies and aromas that are believed to be adaptations for dispersal by insects (CAB International, 2005; Ribeiro, 2005; Al Adawi, *et al*., 2013).

Ceratocystis fimbriata is a complex of many species, each with a unique host range and geographic distribution (CAB International, 2005). In Brazil, Ferreira *et al*. (2010) showed from mating studies and genetic analyses that the limited dispersal distance and a high degree of selfing or asexual reproduction lead to local

populations of *C. fimbriata* that have limited diversity but are highly differentiated from other populations. However, the last years various new species of the *C. fimbriata* complex were distinguished from *C. fimbriata* sensu stricto largely based on variation in ITS rDNA sequences (Harrington *et al*., 2014). But, recently intraspecific and intragenomic variability of ITS rDNA sequences reveals taxonomic problems in *C. fimbriata* sensu strict (Harrington *et al*., 2014). Therefore the taxonomic status of much species delineated primarily by ITS sequences needs further study, but they are considered doubtful species (Harrington *et al*., 2014).

In Brazil, the use of mango cultivars with high levels of resistance to mango wilt has been the most effective strategy adopted by farmers to control the disease, especially because the disease cannot yet be controlled by fungicide (Ribeiro *et al.*, 1986; Rosseto *et al.*, 1996; Ribeiro, 2005). However, due to the great genetic variability of *C. fimbriata*, resistance of mango cultivars may become overcome by other strains of the pathogen (Ribeiro *et al.*, 1986; Rosseto *et al.*, 1996; Ribeiro, 2005). The eradication of mango trees showing mango wilt symptoms can also be used as a strategy to reduce inoculum (Viegas, 1960; Ribeiro, 2005). Insecticide sprays to control insect dispersal are inefficient to minimize the impact of mango wilt (Al Adawi, *et al*., 2013).

A few studies have described the infection process of *Ceratocystis* spp. such as mango-*C. manginecans* (Al-Sadi *et al.*, 2010), eucalyptus-*C. fimbriata* (Ferreira *et al.*, 2005) and American Elm-*C. ulmi* (Shigo and Tippett, 1981). The fungus *Ceratocystis* spp. has been reported as a typical vascular pathogen causing wilting and death of infected trees, due to the occurrence of internal necrosis of the stem tissues and the obstruction of the xylem vessels (Al-Sadi *et al.*, 2010, CAB International, 2005). There are no studies to date explaining how the mango plants respond to *C. fimbriata* infection by examining the inducible defense mechanisms at the vascular system or in other tissues.

The resistance of trees to pathogens is primarily based on their ability to restrict them to a few cells (Duchesne *et al.*, 1992) as showed in studies of compartmentalization of tissues by Shigo and Marx (1977). Suberized bark containing phenolic-like, the composition of the xylem vessels and their diameter are the most common examples of pre-formed mechanisms of host resistance in response to infection by vascular pathogens (Biggs, 1992; Duchesne *et al.*, 1992; Merrill, 1992). In contrast, post-formed defense mechanisms in trees include anatomical

responses, such as the deposition of gels and the formation of tyloses in the vascular vessels; the formation of barrier zones; lignification and suberization of cell walls; and the production of phenolics, phytoalexins and proteins related to the pathogenesis (Blanchette, 1992; Duchesne *et al.*, 1992; Rioux and Baayen, 1997). Generally, defense mechanisms occurring upon wilt pathogen ingress are more efficient at containing the pathogen within a few cells within the host tissue in comparison to pre-formed mechanisms (Merrill, 1992).

Information regarding the infection process of *C. fimbriata* in the stem tissue of mango cultivars and how the host responds in terms of defensive mechanisms at cellular level is lacking in the literature. In this context, this work was divided in two articles. In the first study the objective was to investigate histopathologically how the infection process of two isolates of *C. fimbriata* with different level of aggressiveness can be affected by mango cultivar-specific mechanisms of resistance. Whereas in the second study the objective was to describe and characterize host responses to *C. fimbriata* in stems of resistant and susceptible mango cultivars, with a view of discovering more effective ways to control mango wilt.

REFERENCES

Al Adawi, A.O., Al Jabri, R.M., Deadman, M.L., Barnes, I., Wingfield, B., and Wingfield, M.J. 2013. The mango sudden decline pathogen, *Ceratocystis manginecans*, is vectored by *Hypocryphalus mangiferae* (Coleoptera: Scolytinae) in Oman. Eur. J. Plant Pathol. 135:243-251.

Al-Sadi, A. M., Al-Ouweisi, F. A., Al-Shariani, N. K., Al-Adawi, A. O., Kaplan, E. J., and Deadman, M. L. 2010. Histological changes in mango seedlings following infection with *Ceratocystis manginecans*, the cause of mango decline. J. Phytopathol. 158:738-743.

Biggs, A. R. 1992. Anatomical and physiological responses of bark tissues to mechanical injury. Pages 13-36 in: Defense Mechanisms of Woody Plants Against Fungi. R. A. Blanchette, and A. T. Biggs, eds. Springer-Verlag, Berlin.

Blanchette, R. A. 1992. Anatomical responses of xylem to injury and invasion by fungi. Pages 76-95 in: Defense Mechanisms of Woody Plants Against Fungi. R. A. Blanchette, and A. T. Biggs, eds. Springer-Verlag, Berlin.

CAB International, 2005. *Ceratocystis fimbriata* [original text prepared by T. C. Harrington]. In: Crop protection compendium. Wallingford, UK: CAB International.

Carvalho, C. R. L., Rossetto, C. J., Mantovani, D. M. B., Morgano, M. A., Castro J. V., and Bortoletto N. 2004. Avaliação de cultivares de mangueira selecionadas pelo Instituto Agronômico de Campinas comparadas a outras de importância comercial. Rev. Bras. Frutic. 26:264-271.

Duchesne, L. C., Hubbes, M., and Jeng, R. S. 1992. Biochemistry and molecular biology of defense reactions in the xylem of angiosperm trees. Pages 133-142 in: Defense Mechanisms of Woody Plants Against Fungi. R. A. Blanchette, and A. T. Biggs, eds. Springer-Verlag, Berlin.

FAO, 2013. Medium-term prospects for agricultural Commdities. In: Food and Agriculture Organization of the United Nations. http://www.fao.org/docrep/006/y5143e/y5143e1a.htm.

Ferreira, F.A., Maffia, L.A., Ferreira, E.A. 2005. Detecção rápida de *Ceratocystis fimbriata* em lenho infetado de eucalipto, mangueira e outros hospedeiros lenhosos. Fitopatologia Brasileira 30:543-45.

Ferreira, E. M., Harrington, T. C., Thorpe, D. J., and Alfenas, A. C. 2010. Genetic diversity and interfertility among highly differentiated populations of *Ceratocystis fimbriata* in Brazil. Plant Pathol. 59:721-735.

Harrington, T. C., Kazmi, M. R., Al-Sadi, A. M., and Ismail, S. I. 2014. Intraspecific and intragenomic variability of ITS rDNA sequences reveals taxonomic problems in *Ceratocystis fimbriata* sensu stricto. Mycologia doi:10.3852/13-189.

Merrill, W. 1992. Mechanisms of resistance to fungi in woody plants: A historical perspective. Pages 1-11 in: Defense Mechanisms of Woody Plants Against Fungi. R. A. Blanchette, and A. T. Biggs, eds. Springer-Verlag, Berlin.

Ribeiro, I. J. A. 2005. Doenças da mangueira (*Mangifera indica L.*). Pages 457-465 in: Manual de Fitopatologia: Doenças das Plantas Cultivadas. H. Kimati, L. Amorim, A. Bergamin-Filho, L. E. A. Camargo, and J. A. M. Rezende, eds. Agronômica Ceres, São Paulo.

Ribeiro, S. M. R., Barbosa, L. C. A., Queiroz, J. H., Knodler, M., and Schieber, A. 2008. Phenolic compounds and antioxidant capacity of Brazilian mango (*Mangifera indica* L.) varieties. Food Chem.110:620-626.

Rioux, D., and Baayen, R. P. 1997. A suberized perimedullary reaction zone in *Populus balsamifera* novel for compartmentalization in trees. Trees 11:389-403.

Rossetto, C. J., Ribeiro, I. J. A., Igue, T., and Gallo, P. B. 1996. Seca-da-mangueira XV. Resistência varietal a dois isolados de *Ceratocystis fimbriata*. Bragantia 55:117-121.

Shigo, A.L., and Marx, H.G. (1977) Compartmentalization of decay in trees. USDA For Serv Bull No 405, Washington, D.C.

Shigo, A., and Tippett J.T. 1981. Compartmentalization of American Elm tissues infected by *Ceratocystis ulmi.* Plant Disease 65:715-18.

Viégas, A. P. 1960. Seca da mangueira. Bragantia 19:163-182.

CHAPTER 1

Accepted as original paper to *Plant Pathology*

Histopathological aspects of mango resistance to the infection process of *Ceratocystis fimbriata*

Leonardo Araujo, Wilka Messner Silva Bispo, Isaías Severino Cacique, Maria Fernanda Antunes Cruz and Fabrício Ávila Rodrigues

Viçosa Federal University, Department of Plant Pathology, Laboratory of Host-Pathogen Interaction, Viçosa, Minas Gerais State, Zip Code 36570-900, Brazil

Abstract

Mango wilt, caused by *Ceratocystis fimbriata*, is one of the most important diseases affecting mango yields in Brazil. Information regarding the infection process of *C. fimbriata* in the stem tissues of mango from different cultivars and the basis of host resistance against pathogen infection is scarcely available in the literature. Thus, the objective of the study was to investigate how infection by two isolates of *C. fimbriata* can be affected by mango cultivar-specific mechanisms of resistance. Disease progress on the inoculated stem tissues of the mango cultivars was evaluated and stem sections were obtained from the site of inoculation and prepared for histopathological observations using light microscopy. The factors mango cultivars and *C. fimbriata* isolates and their interaction were significant for all measures of disease development. Plants from the cultivars Espada, Haden and Palmer inoculated with isolates of *C. fimbriata* were more susceptible, whereas plants from the cultivars Tommy and Ubá were moderately resistant and resistant, respectively. Histopathologically, fungal isolates apparently massively colonized the stem tissues of plants from the susceptible cultivars Espada, Haden and Palmer, starting from the collenchyma and moving in the direction of the cortical parenchyma, xylem vessels and pith parenchyma. By contrast, on stem tissues of plants from the resistant cultivars Tommy Atkins and Ubá, most of the cells reacted to *C. fimbriata* infection by accumulating amorphous material. The results from the present study strongly

indicated the importance of phenolic compounds for mango cultivars against the infection of Brazilian *C. fimbriata* isolates.

Keywords: host defense response, light microscopy, mango wilt, phenolics, tylosis, vascular pathogen

Introduction

Mango (*Mangifera indica* L.) is one of the most important tropical fruit crops worldwide. Asia and the Pacific region are the major mango producers, followed by Latin America, the Caribbean and Africa (Food and Agriculture Organization of the United Nations; FAO, 2013). Brazil is the seventh largest mango producer in the world (FAO, 2013) and the cultivars Espada, Haden, Palmer and Tommy Atkins are the most important for fresh consumption, whereas cultivar Ubá has been used for juice production (Carvalho *et al.*, 2004; Ribeiro *et al.*, 2008).

The ability of mango cultivars to adapt to different environmental conditions and to exhibit resistance to multiple diseases are among the factors that have greatly improve yield (Carvalho *et al.*, 2004). Among the diseases affecting mango production, mango wilt, caused by *Ceratocystis fimbriata* Ellis & Halst. (Ferreira *et al.*, 2010; Viégas, 1960) is one of the most important, especially in Brazil (Ribeiro, 2005; Batista *et al.*, 2008). A very similar wilt disease of mango is known in Oman and Pakistan as sudden decline, but it is attributed to *C. manginecans* (Van Wyk *et al.* 2007). *C. fimbriata* causes the death of the entire tree a few months after root penetration or more slowly when the infection takes place on wounded branches of the tree canopy (Batista *et al.*, 2008; Ribeiro, 2005; Viégas, 1960). Typical symptoms of mango wilt include wilting and browning of the leaves on single branches and gum exudation from the trunks (Ribeiro, 2005; Viégas, 1960). The external and internal stem tissues become dark brown upon infection by *C. fimbriata* (Ribeiro, 2005; Viégas, 1960). Some populations of *C. fimbriata* infecting mango are highly differentiated from other geographically isolated populations (Ferreira *et al.*, 2010), resulting in differences in fungal aggressiveness (Batista *et al.*, 2008; Ribeiro, 2005; Rossetto *et al.*, 1996).

Host resistance is the most common strategy to control mango wilt, especially because no fungicides have been registered to control this disease in Brazil (Batista *et al.*, 2008; Ribeiro, 2005). However, due to the significant genetic variability of *C. fimbriata*, resistant cultivars may become susceptible over time (Ribeiro *et al.*, 1986; Ribeiro, 2005). The eradication of mango trees showing mango wilt symptoms can also be used as a strategy to slow the progression of disease (Ribeiro, 2005; Viégas, 1960).

A few studies have described the process by which *Ceratocystis* spp. infect susceptible hosts. This includes studies of the mango-*C. manginecans* (Al-Sadi *et al.*,

2010), eucalyptus-*C. fimbriata* (Ferreira *et al.*, 2005) and American Elm-*C. ulmi* (Shigo & Tippett, 1981) pathosystems. The fungus *Ceratocystis* spp. has been reported in the literature as a typical vascular pathogen causing wilting and death of infected trees due to the occurrence of internal necrosis of the stem tissues and the obstruction of the xylem vessels (Al-Sadi *et al.*, 2010, CAB International, 2005). There are no studies to date explaining how the mango plants respond to *C. fimbriata* infection by examining the inducible defense mechanisms at the vascular system level or in other tissues.

In general, tree's resistance to pathogens is based on its ability to confine them to a few cells (Duchesne *et al.*, 1992). Suberized bark containing phenolic compounds, the composition of the xylem vessels and their diameter are the most common examples of pre-formed mechanisms of host resistance in response to wilt pathogen infection (Biggs, 1992; Duchesne *et al.*, 1992; Merrill, 1992). In contrast, induced host defense mechanisms include anatomical responses such as the deposition of gels and/or tyloses in the vascular system; cell wall lignification and suberization; and the synthesis of phenolics, phytoalexins and proteins related to pathogenesis (Duchesne *et al.*, 1992).

Generally, defense mechanisms occurring upon wilt pathogen ingress are more effective than pre-formed mechanisms at containing the pathogen within a few cells of host tissue (Merrill, 1992). Shigo and Tippett (1981) reported the formation of a barrier zone that separated the xylem vessels infected by *C. ulmi* from the healthy xylem vessels on the cambium of stem tissues of a resistant cultivar of American Elm. Eynck *et al.* (2009) found a positive relationship between the abundance of vascular occlusions (vascular gels and tyloses) and the level of resistance of oilseed rape to *Verticillium longisporum*. Intense lignification of root tissues from resistant tomato seedlings restricted the colonization by *Fusarium oxysporum* f.sp. *radicis-lycopersici* (Benhamou & Bélanger, 1998). The accumulation of suberin in callus cultures of *Ulmus americana* infected by *Ophiostoma novo-ulmi* was almost five folds higher in the inoculated than in the water-treated callus, indicating that suberization is an important mechanism to avoid pathogen spread (Aoun *et al.*, 2009). According to Hall *et al.* (2011), the accumulation of amorphous materials, identified as terpenoid phytoalexins, in the xylem vessels and in adjacent parenchyma cells in roots of a cotton resistant cultivar restricted colonization by *F. oxysporum vasinfectum*.

Information regarding the infection process of *C. fimbriata* in the stem tissues of mango, especially from different cultivars, and the basis of host resistance against pathogen infection at the vascular system level is scarcely available in the literature (Al-Sadi *et al.*, 2010; Ribeiro *et al.*, 1986). Thus, the objective of the present study was to investigate histopathologically how the infection process of two isolates of *C. fimbriata* with different level of aggressiveness can be affected by mango cultivar-specific mechanisms of resistance.

Materials and methods

Plant material

Mango plants from the cultivars Espada, Haden, Palmer, Tommy Atkins and Ubá were obtained from a commercial orchard (Dona Euzébia city, Minas Gerais State, Brazil). The 1 ½ year-old plants were transplanted into plastic pots containing 8 kg of substrate consisting of a mixture of soil, sand and manure in the proportion of 2:1:1. The five mango cultivars were used as the canopy, whereas the cultivar Imbú was used as their rootstock. Plants were kept in the greenhouse (temperature of 30 ± 2°C and relative humidity of 70 ± 5%) for 2 months before the beginning of the experiments. Plants were irrigated as needed.

Inoculation procedure

C. fimbriata isolates, CEBS15 and MSAK16, obtained from symptomatic mango plants collected in the cities of Brejo Santo and Aquidauana located in the States of Ceará and Mato Grosso do Sul, respectively, in Brazil, were used to inoculate mango plants. The isolates were preserved by Castellani's method (Dhingra & Sinclair, 1995). Plugs of malt-extract-agar (MEA) medium containing fungal mycelia were transferred to Petri dishes containing potato-dextrose-agar (PDA). After three days, PDA plugs containing fungal mycelia were transferred to Petri dishes containing the same culture medium and incubated at 25°C and 12 h photoperiod for 14 days.

The inoculation procedure was performed according to Al-Sadi *et al.* (2010) with a few modifications. Bark disks (10 mm in diameter and 2 mm height) were removed from the stems of plants from the five cultivars with the aid of a punch at approximately 5 cm above the graft scar. A PDA plug (10 mm in diameter) obtained from 14-day-old colonies of each *C. fimbriata* isolate was placed in the wound made with a punch. Each wound containing the PDA plug with fungal mycelia was carefully covered with a piece of moistened cotton and then covered with parafilm to maintain adequate moisture for fungal infection. PDA plug used to inoculate plants were taken from the middle portion of each fungal colony to make the inoculation as homogeneous as possible. Wound on the stems of plants receiving only plugs of PDA medium served as the control.

Disease assessments

Disease progress, including lesion development and wilting of the leaves of the inoculated plants were evaluated at 15, 22 and 29 days after inoculation (dai). The upward, downward and radial colonization of stem tissues by fungal hyphae of the

two isolates of *C. fimbriata* were evaluated by measuring the length (in cm) of the internal necrotic tissue using digital calipers. The upward relative lesion length (URLL) and the downward relative lesion length (DRLL) were determined as the ratio between the length from the graft scar to the top of the stem (LGST) and the lesion length (LL) in the same interval (upward and downward) from the inoculation point according to the following formula: URLL or DRLL = LL × 100/LGST. The plants were standardized to a length of 20 cm (distance from the graft scar to the top of the stem). The radial fungal colonization (RFC) was determined as the length of the necrotic tissue in relation to the total stem diameter × 100. Symptoms of internal necrotic tissues in both longitudinal and transverse stem sections obtained from the five cultivars inoculated with the two isolates of *C. fimbriata* were photographed (6.5 × for the whole stem tissue and 40 × to show stem tissue-associated perithecia) under a stereomicroscope (Stemi 2000-C, Carl Zeiss, Germany) coupled with a digital camera (PowerShot A640, Canon). The percentage of wilted leaves from the total number of leaves per plant of each cultivar was determined according to Al-Sadi *et al.* (2010). Representative mango plants of the five cultivars infected with the two isolates of *C. fimbriata* were digitally photographed (Coolpix L110, Nikon) at each sampling time to record the pattern of wilting development. Data from URLL, DRLL, RFC and the percentage of wilted leaves were used, respectively, to calculate the area under the upward relative lesion length progress curve (AUURLLPC), area under the downward relative lesion length progress curve (AUDRLLPC), area under the radial fungal colonization progress curve (AURFCPC) and area under the wilted leaves progress curve (AUWLPC) according to Shaner and Finney (1977).

Processing infected stem tissues for light microscopy

A total of 25 to 30 longitudinal and transverse stem sections of three plants from the five cultivars (10 mm thick) were obtained from three cm below and above the inoculation point at 15, 22 and 29 dai with the two *C. fimbriata* isolates. Sections taken from the stems of noninoculated plants served as the control treatment. Stem sections were carefully transferred to glass vials and fixed with 10 ml of a fixative composed of 3% (v/v) glutaraldehyde and 2% paraformaldehyde (v/v) in 0.1 M sodium cacodylate buffer (pH 7.2) and stored at 4°C for two months (Rodrigues *et al.*, 2003). In the next step, samples were carefully washed with 0.1 M sodium cacodylate buffer, subsequently dehydrated through a graded alcohol series (10, 30, 50, 70, 85, 95 and 100%) and embedded in methacrylate resin (Historesin, Leica,

Nussloch, Heidelberg, Germany). During the preinfiltration and infiltration steps, samples were placed in a vacuum chamber for 2 h both in the morning and in the afternoon for three weeks to allow better resin infiltration into the stem tissues. The samples were stored at 4°C after each vacuum procedure. A total of six blocks containing two stem fragments were obtained for each treatment at each sampling time. Longitudinal and transverse serial sections (1 μm thick) were cut from each block using a Leica RM 2245 rotary microtome (Leica Microsystems®, Nussloch, Germany) and stained with 1% toluidine blue in 2% sodium borate for 5 min. A total of 48 sections of infected stem fragments were obtained per block, which were randomly divided into four glass slides. Images of the details regarding fungal infection and host defense responses were acquired digitally (Axio Cam HR, Carl Zeiss) in bright-field mode with a Carl Zeiss Axio Imager A1 microscope (Carl Zeiss, Germany) and further processed with the software Axion Vision 4.8.1.

Experimental design

A 5 × 2 factorial experiment consisting of mango cultivars (Espada, Haden, Palmer, Tommy Atkins and Ubá) and *C. fimbriata* isolates (CEBS15 and MSAK16) was arranged in a completely randomized design with four replications. Each replication consisted of a plastic plot containing one mango plant. The experiment was repeated once. Data for AUWLPC was transformed to square root of x before statistical analysis. The data were analyzed by an analysis of variance (ANOVA) and treatments means comparisons by Tukey's test ($P \leq 0.05$) using SAS (Release 8.02 Level 02M0 for Windows, SAS Institute, Inc., 1989, Cary, NC, USA).

Results

Disease assessments

The factors mango cultivars and *C. fimbriata* isolates and their interaction were significant for AUURLLPC ($P \leq 0.01$), AUDRLLPC ($P \leq 0.01$), AURFCPC ($P \leq 0.01$) and AUWLPC ($P \leq 0.01$) (Table 1). Mango plants from the cultivars Espada, Haden and Palmer inoculated with *C. fimbriata* isolate CEBS15 were more susceptible than cultivars Tommy and Ubá based on the AUURLLPC ($P \leq 0.01$) and AUWLPC ($P \leq 0.01$) values (Table 1). There was no significant difference between the cultivars regarding the AUDRLLPC ($P = 0.35$) (Table 1). The AURRLLPC was significantly higher for cultivars Espada and Palmer compared to cultivar Ubá, whereas the Haden and Tommy cultivars showed intermediate values ($P \leq 0.05$) (Table 1). Mango plants from the cultivars Espada and Haden inoculated with *C. fimbriata* isolate MSAK16 were more susceptible than Ubá based on the AUURLLPC ($P \leq 0.01$), AUDRLLPC ($P \leq 0.05$), AURFCPC ($P \leq 0.01$) and AUWLPC ($P \leq 0.01$) values (Table 1). The cultivars Palmer and Tommy showed variations in their level of resistance to MSAK16 according to the method of disease assessment (Table 1). Isolate CEBS15 was more aggressive compared to isolate MSAK16 on plants from cultivars Palmer ($P \leq 0.05$) and Ubá ($P \leq 0.01$) (Table 1). Isolate MSAK16 was more aggressive on plants of cultivar Haden ($P \leq 0.05$) (Table 1). The two isolates of *C. fimbriata* showed variations in their level of aggressiveness when inoculated on plants of cultivars Espada and Tommy based on the AURRLLPC and AUWLPC values (Table 1).

Stem tissues obtained from plants of cultivars Espada, Haden and Palmer showed more internal necrosis regardless of *C. fimbriata* isolate compared with stem tissues obtained from plants of cultivars Tommy and Ubá (Figs. 1). Perithecia formed by the two isolates of *C. fimbriata* were observed at the inoculation point of stem tissues of all mango cultivars at 22 dai (Figs. 1A, E and I). The first symptoms of wilted leaves on plants from cultivars Espada and Palmer, appear on branches closer from the inoculation point with or without leaf blight occurred at 13 dai with the two isolates of *C. fimbriata* (Figs. 2C and G). At 22 dai, various levels of wilting were observed on plants from all cultivars, except Ubá that not exhibit symptoms (Figs. 2I and J). At 22 and 29 dai, some plants from cultivars Espada, Haden and Palmer had died. Dead plants and plants with intense wilting exhibited external necrotic stem tissue (Fig. 2A). Plants from cultivar Palmer did not wilt when infected with isolate

MSAK16 (Fig. 2F). On plants from cultivar Tommy, the wilting was mild when inoculated with isolate CEBS15 (Fig. 2G), but not exhibit symptoms when inoculated with MSAK16.

Light microscope observations

Colonization of the stem tissues of plants from susceptible and resistant cultivars by *C. fimbriata*

Examination of several longitudinal and transverse stem tissue sections at 22 dai using a light microscope confirmed the visual differences observed in the pattern of internal stem necrosis and wilting. The two isolates of *C. fimbriata* colonized the stem tissues of plants from the susceptible (Espada, Haden and Palmer), moderately resistant (Tommy Atkins) and resistant (Ubá) mango cultivars starting from the collenchyma and toward the cortical parenchyma, xylem vessels and pith parenchyma (Figs. 3, 4, 5, 6 and 7).

Colonization of collenchyma

Fungal hyphae of the two *C. fimbriata* isolates apparently did not grow well in the collenchyma of plants of any of the cultivars (Fig. 3, 4, 5, 6 and 7). Fungal hyphae that colonized the collenchyma cells were frequently surrounded by an amorphous granular material that stained densely with toluidine blue (Figs. 3G, 4C, 6C and 7C). In some cells, fungal hyphae appeared as empty shells (Figs. 4C, 6C and 7C).

Colonization of cortical parenchyma

Fungal hyphae of *C. fimbriata* isolates apparently grew without any impedance in the cortical parenchyma of stem tissues of plants from the susceptible cultivars Espada, Haden and Palmer (Figs. 3, 4 and 5). In some cells, amorphous granular material was scarcely deposited around fungal hyphae (Figs. 3, 4 and 5). Large chlamydospores (aleurioconidia) and long, thickened fungal hyphae were observed in the cells of the medullary radius and parenchyma of stem tissues from plants of the susceptible cultivars Espada, Haden and Palmer (Figs. 3, 4 and 5). In the stem tissues of plants from cultivar Palmer, more cortical parenchyma cells were observed to be colonized by fungal hyphae of isolate MSAK16, which reacted by accumulating amorphous material that stained dark blue or purple (Figs. 5I and K), compared to isolate CEBS15 (Fig. 5D). Occasionally, fungal hyphae of isolate MSAK16 appeared as empty shells in the stem tissues of plants from cultivar Palmer (Fig. 5K). In the stem tissues of plants from cultivars Espada and Palmer, not yet colonized by fungal hyphae of the isolates CEBS15 and MSAK16, respectively, the plasmatic membrane

of some fiber and parenchyma cells were detached, indicating possible cell death (Figs. 3E, 5I and 8K).

On plants from the moderately resistant (Tommy Atkins) and resistant cultivar (Ubá), most cells of the cortical parenchyma colonized by fungal hyphae of the two *C. fimbriata* isolates reacted strongly to fungal invasion by deposition of an amorphous granular material (Figs. 6 and 7) or were stained intense dark blue or purple (Figs. 6A, B, 7A and B). In these cells, fungal hyphae frequently appeared as empty shells (Figs. 6H and J; 7D, F, H, I and J) or were thin and faint (Figs. 6 and 7) and few chlamydospores were found (Figs. 7D). For both *C. fimbriata* isolates, fungal hyphae appearing as empty shells were more apparent in cultivar Uba than Tommy Atkins (Figs. 6 and 7). When comparing fungal isolates on plants from cultivar Uba, hyphae from isolate MSAK16, appearing as empty shells, was more commonly observed (Figs. 7D, E, F, H, I and K).

Colonization of xylem vessels

On the stem tissues of plants from susceptible cultivars Espada, Haden and Palmer, fungal hyphae of two isolates of *C. fimbriata* reached the xylem vessels, stimulating intense formation of polysaccharide gels and tyloses (Figs. 3, 4 and 5). Xylem vessels in the stem tissues of plants from cultivars Espada and Haden were observed to be more obstructed by deposition of polysaccharide gels, fungal hyphae, chlamydospores and tyloses when infected by isolate MSAK16 (Figs. 3H and I; 4J and K) in comparison to CEBS15 (Figs. 3C and E; 4D and F). Chains of chlamydospores were observed in the xylem vessels of plants from cultivar Haden inoculated with isolate MSAK16 (Figs. 4H, I and K). In the stem tissues of plants from cultivar Palmer, xylem vessels were commonly obstructed when inoculated with isolate CEBS15 (Figs. 5C, E, F, H, I and J).

Fungal hyphae of the two isolates of *C. fimbriata*, were thin and faint in their appearance and were rarely observed to reach xylem vessels in the stem tissues of plants from moderately resistant and resistant mango cultivars Tommy Atkins and Ubá, respectively (Figs. 6D, G and I; 7E and H). Xylem vessels in stem tissues of plants from the resistant cultivars were free of any occlusions (Figs. 6D, G, I and J; 7E and I) or were fully obstructed by large tyloses that stained dark blue or purple, indicating the presence of phenolic compounds (Figs. 6E; 7D and H). No visual differences were observed between *C. fimbriata* isolates on plants from the moderately resistant and resistant cultivars (Figs. 6 and 7).

Colonization of pith parenchyma

The two *C. fimbriata* isolates extensively colonized the pith parenchyma in the radial direction in the stem tissues of plants from the susceptible cultivars Espada, Haden and Palmer (Figs. 3, 4 and 5). Some cells reacted to fungal invasion by accumulating amorphous granular material (Figs. 3F and J; 4G and L; 5G and L). In the cells of pith parenchyma on the stem tissues of plants from cultivar Palmer, some fungal hyphae appeared as empty shells (Figs. 5G and L). Fungal hyphae of the isolates MSAK16 and CEBS15 grew in the pith parenchyma in the radial direction, reaching again the xylem vessels in the stem tissues of plants from cultivars Haden (Fig. 4B) and Palmer (Fig. 5A), respectively. Fungal hyphae of isolate CEBS15 were more frequently observed in the pith parenchyma in stem tissues of plants from cultivars Espada and Palmer compared with isolate MSAK16 (Figs. 3A and B; 5A and B). However, in the stem tissues of plants from cultivar Haden, fungal hyphae of isolate MSAK16 apparently grew more in the pith parenchyma (Figs. 4A and B).

Fungal hyphae of the two *C. fimbriata* isolates apparently scarcely colonized the pith parenchyma in the radial direction in the stem tissues of plants from the moderately resistant and resistant cultivars Tommy Atkins and Ubá (Figs. 6A, B, F and K and 7A, B, G and K). Most of the cells reacted to *C. fimbriata* infection, regardless of the isolate, by accumulating amorphous granular material that surrounded many fungal hyphae, which sometimes appeared thin and faint or as empty shells (Figs. 6F and K; 7G and K). In the stem tissues of plants from cultivar Tommy, more extensive growth of MSAK16 was observed in the pith parenchyma compared to that of isolate CEBS15 (Figs. 6A, B, F and K). By contrast, in stem tissues of plants from cultivar Ubá, CEBS15 apparently grew more extensively in the pith parenchyma than did isolate MSAK16 (Figs. 7A, B, G and K).

Discussion

This study provides, to the best of our knowledge, the first direct evidence that mango cultivars respond differently to the infection by *C. fimbriata* at the cellular level according to their basal level of resistance. The AURFCPC and AUWLPC provided the best separation of the five cultivars according to their levels of resistance to mango wilt. High values of AURFCPC and AUWLPC were associated with death of the susceptible mango plants cultivars. External and internal necrotic tissues in the stem of plants are the major symptoms of mango wilt prior to complete wilting (Ribeiro, 2005; Viégas, 1960). Park *et al.* (2013) showed that a high proportion of external necrotic tissues on the stem of hickory trees infected with *C. smalleyi* contributed to xylem dysfunction and resulted in wilting symptoms and decline of plants. In the present study, the lowest values for almost all measures of disease development were obtained for plants from cultivars Tommy Atkins and Ubá, which did not show intense wilting and death of plants until the end of the experiment.

A few studies have reported that *Ceratocystis* spp. colonizes mainly the vascular system of various plant species (Al Sadi *et al.*, 2010; Ferreira *et al.*, 2005; Park *et al.*, 2013). According to Al Sadi *et al.* (2010), hyphae of *C. manginecans* were only found in the vascular system of inoculated mango seedlings. Ferreira *et al.* (2005) found hyphae of *C. fimbriata* in the vascular system and in the pith parenchyma of *Eucalyptus* plants. In contrast, Viégas (1960) was the first to suggest that *C. fimbriata* is not an exclusive vascular pathogen because the xylem vessels were not completely obstructed with fungal hyphae, as in *Verticillium*-cotton pathossystem. Results from the present study clearly show that isolates of *C. fimbriata* obtained in Brazil colonized all stem tissues of mango cultivars, and therefore it, cannot be considered an exclusive vascular pathogen as reported in the literature.

Most pathogenic fungi do not extensively colonize collenchyma cells due to the presence of many phenolic compounds (Merrill, 1992; Kim *et al.*, 2004). This proved to be the case also for *C. fimbriata*, which we found rarely to be present in collenchyma cells. Fungal hyphae that were observed in collenchyma cells were frequently encased by an amorphous material that stained densely with toluidine blue, indicating the presence of phenolics. The accumulation of amorphous materials is a typical feature of the cellular defense of many plant species against pathogenic fungi (Ajila *et al.*, 2010; Bélanger *et al.*, 2003; Benhamou & Bélanger, 1998; Eynck

et al., 2009; Hall *et al.*, 2011; Kim *et al.*, 2004; Rodrigues *et al.*, 2003). Pre-formed or induced phenolic compounds play an important role in host defense against pathogen infection (Nicholson & Hammerschmidt, 1992) such as in cell wall lignification (Benhamou & Bélanger, 1998), in antimicrobial activity (Rodrigues *et al.*, 2003), as modulators of plant hormones in defense signaling and as scavengers of reactive oxygen species (Dixon & Paiva, 1995). In the present study, the scarcity of fungal hyphae in collenchyma cells may have been, due to the intense deposition of phenolic compounds in these cells.

Fungal hyphae of *C. fimbriata* apparently grew without any impedance in the cortical parenchyma and xylem vessels of stem tissues of susceptible cultivars. By contrast, in stems of moderately resistant and resistant cultivars, most cells reacted to *C. fimbriata* infection by accumulating amorphous material that contributed to many fungal hyphae appearing as empty shells. Several other studies have also reported the occurrence of empty fungal hyphae of pathogens surrounded by amorphous material in the cells of many plant species (Bélanger *et al.*, 2003; Benhamou & Bélanger, 1998; Ouellette *et al.*, 1992; Rodrigues *et al.*, 2003). Eynck *et al.* (2009) observed intense deposition of phenolics and lignin compounds in the cells of roots and hypocotyls of resistant oilseed rape plants in response to infection by *V. longisporum* compared to the tissues of susceptible plants. In the present study, intense deposition of amorphous material surrounding fungal hyphae of both fungal in the cortical parenchyma and xylem vessels helped to explain limited disease development on plants from cultivars Tommy Atkins and Ubá.

Intense deposition of phenolic compounds was also noted on the parenchyma cells adjacent to the xylem vessels on the stems of plants from the resistant mango cultivars. Similarly, deposition of phenolic compounds in the parenchyma cells surrounding the xylem vessels in cotton plants was regarded as a barrier to colonization by *F. oxysporum vasinfectum* (Hall *et al.*, 2011; Shi *et al.*, 1992). In the barrier zones formed in response to pathogens infection, suberin, phytoalexins, phenolics and lignin are of great importance (Shigo & Tippett, 1981; Ouellette & Rioux, 1992). The deposition of phenolics in the barrier zones is also an efficient defense mechanism to avoid the colonization of the wilt pathogens *C. ulmi* and *O. novo-ulmi* in the stem tissues of American Elm (Aoun *et al.*, 2009; Shigo & Tippett, 1981). In the present study, the intense deposition of phenolic compounds on the parenchyma cells adjacent to the xylem vessels may have contributed as antifungal

barrier that impeded the greater colonization of the vascular system on the stems of plants from the moderately resistant and resistant cultivars in comparison to tissues of plants from the susceptible cultivars.

In the stem tissues of plants from the susceptible cultivars, hyphae of *C. fimbriata* reached the xylem vessels and stimulated the formation of intense polysaccharide gels and many tyloses. By contrast, in moderately resistant and resistant cultivars, vessels were free of any occlusions, including fungal hyphae, or were fully obstructed by many large tyloses and phenolic compounds. Gels and tyloses are good examples of occluding structures produced by plants that serve to impede tissue colonization by wilt pathogens (Duchesne *et al.*, 1992; Rioux *et al.*, 1998). These occluding structures can be effective whether produced in advance of fungal ingress or during the colonization process (Ouellette & Rioux, 1992). Williams *et al.* (2002) and Eynck *et al.* (2009) reported a positive relationship between the abundance of vascular occlusions (gels and tyloses) and the increased level of resistance on the stem tissues of tomato and oilseed rape plants to infection by *Verticillium* spp. In contrast, Park *et al.* (2013) observed that the accumulation of gels and tyloses in the xylem vessels contributed to reduced sap flow at the margin of the necrotic sapwood of bitternut hickory infected by *C. smalleyi*. According to Al Sadi *et al.* (2010), tyloses and hyphae of *C. manginecans* in the vascular system were responsible for the wilting and the death of mango seedlings. In the present study, differences in the susceptibility of the mango cultivars to *C. fimbriata* could be attributable to differences in the ability of plants to prevent rapid pathogen colonization of the xylem vessels by quick deposition of tyloses impregnated with phenolic compounds.

The intense formation of polysaccharide gels in the xylem vessels of stem tissues of the susceptible mango cultivars did not appear to be involved in resistance to *C. fimbriata.* It has been reported that gel formation in the xylem vessels of plants infected by vascular pathogens might arise from the swelling of the pit membranes, vessel perforation plates and/or by material secreted from parenchyma cells adjacent to the xylem vessels through membranes of half-bordered pit pairs and by the action of pectolytic enzymes produced by the pathogens (Ouellette & Rioux, 1992; Rioux *et al.*, 1998). Uritani and Stahmann (1961) reported that *C. fimbriata* produces pectinases in the culture media and in the penetrated cells of sweet potato. In the present study, the intense formation of polysaccharide gels in the xylem vessels are

probably due to the degradation of cell wall of stem tissues of plants from the susceptible cultivars by the action of pectolytic enzymes released by *C. fimbriata*.

Many chlamydospores of *C. fimbriata* were observed in the xylem vessels and parenchyma cells of stem tissues from plants of the susceptible cultivars. *Ceratocystis fimbriata* has specialized conidiophores that give rise the chlamydospores also called aleurioconidia that are pigmented, thick-walled, and filled with nutrient reserves substance (Viegas, 1960; CAB International, 2005; Paulin-Mahady *et al*., 2002). Chlamydospores are durable structures that allow the pathogen to survive in the absence of a susceptible host (CAB International, 2005; Paulin-Mahady *et al*., 2002). Ferreira *et al.* (2005) also found most chlamydospores, simple or in chains, of *C. fimbriata* in the xylem vessels, medullary rays and pith parenchyma of *Eucalyptus* plants.

Ceratocystis fimbriata extensively colonized the pith parenchyma in stem tissues of plants from the susceptible mango cultivars in the radial direction, whereas in the moderately resistant and resistant cultivars, fungal hyphae scarcely reached these cells. Similarly, colonization of the xylem vessels of plants from a resistant cotton cultivar by *F. oxysporum* f.sp. *vasinfectum* was reduced by the accumulation of phenolic compounds, with the number of infected xylem vessels decreasing as the distance from the inoculation point increased (Shi *et al.*, 1992). By contrast, in the susceptible plants, *F. oxysporum* f.sp. *vasinfectum* colonized both longitudinal and lateral stem tissues and the defense mechanism occurring in the cells against fungal infection was delayed and weak (Shi *et al.*, 1992). In the present study, accumulation of phenolic compounds probably contributed to diminished colonization by *C. fimbriata* in the upward, downward and radial direction and helped to explain the lower values for the AURFCPC and AUWLPC for the resistant cultivars.

Acknowledgements

Prof. F. A. Rodrigues thanks CNPq for his fellowship. Mr. L. Araujo was supported by CNPq. The authors thank Prof. A. C. Alfenas and Mr. L. S. S. Oliveira for kindly providing the two isolates of *C. fimbriata* used in this study. We thank Mr. W. R. Moreira for technical assistance. This study was supported by a grant from Vale S.A. to Prof. F. A. Rodrigues.

References

Ajila CM, Rao LJ, Rao UJSP, 2010. Characterization of bioactive compounds from raw and ripe *Mangifera indica* L. peel extracts. *Food and Chemical Toxicology* **48,** 3406-11.

Al-Sadi AM, Al-Ouweisi FA, Al-Shariani NK, Al-Adawi AO, Kaplan EJ, Deadman ML, 2010. Histological changes in mango seedlings following infection with *Ceratocystis manginecans*, the cause of mango decline. *Journal of Phytopathology* **158,** 738-43.

Aoun M, Rioux D, Simard M, Bernier L, 2009. Fungal colonization and host defense reactions in *Ulmus americana* callus cultures inoculated with *Ophiostoma novo-ulmi*. *Phytopathology* **99,** 642-50.

Bélanger RR, Benhamou N, Menzies JG, 2003. Cytological evidence of an active role of silicon in wheat resistance to powdery mildew (*Blumeria graminis* f.sp. *tritici*). *Phytopathology* **93,** 402-12.

Benhamou N, Bélanger RR, 1998. Benzothiadiazole-mediated induced resistance to *Fusarium oxysporum* f.sp. *radicis-lycopersici* in tomato. *Plant Physiology* **118,** 1203-12.

Batista DC, Terao D, Barbosa MAG, Barbosa FR, 2008. Seca-da-mangueira: detecção, sintomatologia e controle, Publicado online pela Empresa Brasileira de Pesquisa Agropecuária Semi-árido. Arquivo n. 138. http://www.cpatsa.embrapa.br/ public_eletronica/downloads/COT138. Acess 01 06 2013.

Biggs AR, 1992. Anatomical and physiological responses of bark tissues to mechanical injury. In: Blanchette RA, Biggs AT, eds. *Defense Mechanisms of Woody Plants Against Fungi*. Springer-Verlag, Berlin, 13-36

CAB International, 2005. *Ceratocystis fimbriata* [original text prepared by T. C. Harrington]. In: Crop protection compendium. Wallingford, UK: CAB International. Carvalho CRL, Rossetto CJ, Mantovani DMB, Morgano MA, Castro JV, Bortoletto N, 2004. Avaliação de cultivares de mangueira selecionadas pelo Instituto Agronômico de Campinas comparadas a outras de importância comercial. *Revista Brasileira de Fruticultura* **26,** 264-71.

Dhingra OD, Sinclair JB, 1995. Basic Plant Pathology Methods. Boca Raton, Lewis Publisher.

Dixon RA, Paiva NL, 1995. Stress induced phenylpropanoid metabolism. *Plant Cell* **7,** 1085-97.

Duchesne LC, Hubbes M, Jeng RS, 1992. Biochemistry and molecular biology of defense reactions in the xylem of angiosperm trees. In: Blanchette RA, Biggs AT, eds. *Defense Mechanisms of Woody Plants Against Fungi*. Springer-Verlag, Berlin, 133-42.

Eynck C, Koopmann B, Karlovsky P, von Tiedemann A, 2009. Internal resistance in winter oilseed rape inhibits systemic spread of the vascular pathogen *Verticillium longisporum*. *Phytopathology* **99,** 802-11.

FAO, 2013. Medium-term prospects for agricultural Commdities. In: Food and Agriculture Organization of the United Nations. http://www.fao.org/docrep/006/y5143e/y5143e1a.
htm.

Ferreira EM, Harrington TC, Thorpe DJ, Alfenas AC, 2010. Genetic diversity and interfertility among highly differentiated populations of *Ceratocystis fimbriata* in Brazil. *Plant Pathology* **59,** 721-35.

Ferreira FA, Maffia LA, Ferreira EA, 2005. Detecção rápida de *Ceratocystis fimbriata* em lenho infetado de eucalipto, mangueira e outros hospedeiros lenhosos. *Fitopatologia Brasileira* **30,** 543-45.

Hall C, Heath R, Guest DI, 2011. Rapid and intense accumulation of terpenoid phytoalexins in infected xylem tissues of cotton (*Gossypium hirsutum*) resistant to *Fusarium oxysporum* f.sp. *vasinfectum. Physiological and Molecular Plant Pathology* **76,** 182-88.

Kim KH, Yoon JB, Park HG, Park EW, Kim YH, 2004. Structural modifications and programmed cell death of chili pepper fruit related to resistance responses to *Colletotrichum gloeosporioides* infection. *Phytopathology* **94,** 1295-1304.

Merrill W, 1992. Mechanisms of resistance to fungi in woody plants: A historical perspective. In: Blanchette RA, Biggs AT, eds. *Defense Mechanisms of Woody Plants Against Fungi*. Springer-Verlag, Berlin, 1-11.

Nicholson RL, Hammerschmidt R, 1992. Phenolic compounds and their role in disease resistance. *Annual Review of Phytopathology* **30,** 369-89.

Ouellette GB, Rioux D, 1992. Anatomical and physiological aspects of resistance to Dutch Elm disease. In: Defense Mechanisms of Woody Plants Against Fungi. R. A. Blanchette, and A. T. Biggs, eds. Springer-Verlag, Berlin, 257-301.

Park JH, Juzwik J, Cavender-Bares J, 2013. Multiple *Ceratocystis smalleyi* infections associated with reduced stem water transport in bitternut hickory. *Phytopathology* **103,** 565-74.

Ribeiro IJA, Rossetto CJ, Sabino JC, Gallo PB, 1986. Seca da mangueira: VIII. Resistência de porta-enxertos de mangueira ao fungo *Ceratocystis fimbriata* Ell. & Halst. *Bragantia* **45,** 317-22.

Ribeiro IJA, 2005. Doenças da mangueira (*Mangifera indica L.*). In: Kimati H, Amorim L, Bergamin-Filho A, Camargo LEA, Rezende JAM, eds. *Manual de Fitopatologia: Doenças das Plantas Cultivadas.* Agronômica Ceres, São Paulo, 457-65.

Ribeiro SMR, Barbosa LCA, Queiroz JH, Knodler M, Schieber A, 2008. Phenolic compounds and antioxidant capacity of Brazilian mango (*Mangifera indica* L.) varieties. *Food Chemistry* **110,** 620-26.

Rioux D, Nicole M, Simard M, Ouellette GB, 1998. Immunocytochemical evidence that secretion of pectin occurs during gel (gum) and tylosis formation in trees. *Phytopathology* **88,** 494-505.

Rodrigues FA, Benhamou, N, Datnoff LE, Jones JB, Bélanger RR, 2003. Ultrastructural and cytochemical aspects of silicon-mediated rice blast resistance. *Phytopathology* **93,** 535-46.

Rossetto CJ, Ribeiro IJA, Igue T, Gallo PB, 1996. Seca-da-mangueira: XV. Resistência varietal a dois isolados de *Ceratocystis fimbriata*. *Bragantia* **55,** 117-21.

Shaner G, Finney RE, 1977. The effect of nitrogen fertilization on the expression of slow-mildewing resistance in knox wheat. *Phytopathology* **70,** 1183-86.

Shi J, Mueller WC, Beckman CH, 1992. Vessel occlusion and secretory activities of vessel contact cells in resistant or susceptible cotton plants infected with *Fusarium oxysporum* f.sp. *vasinfectum. Physiological and Molecular Plant Pathology* **40,** 133-47.

Shigo A, Tippett JT, 1981. Compartmentalization of American Elm tissues infected by *Ceratocystis ulmi. Plant Disease* **65,** 715-18.

Uritani I, Stahmann MA, 1961. Pectolytic enzymes of *Ceratocystis fimbriata*. *Phytopathology* **51,** 277-85.

Van Wyk M, Al Adawi AO, Khan IA, Deadman ML, Al Jahwari AA, Wingfield BD, Ploetz R, Wingfield MJ, 2007. *Ceratocystis manginecans* sp. nov., causal agent

of a destructive mango wilt disease in Oman and Pakistan. *Fungal Diversity* **27**, 213-30.

Viégas AP, 1960. Seca da mangueira. *Bragantia* **19,** 163-82.

Williams JS, Hall SA, Hawkesford MJ, Beale MH, Cooper RM, 2002. Elemental sulfur and thiol accumulation in tomato and defense against a fungal vascular pathogen. *Plant Physiology* **128,** 150-9.

LIST OF TABLE AND FIGURES

Table 1 Area under upward relative lesion length progress curve (AUURLLPC), area under downward relative lesion length progress curve (AUDRLLPC) and area under radial fungal colonization progress curve (AURFCPC) on stem tissues and area under wilted leaves progress curve (AUWLPC) in five mango cultivars inoculated with the isolates CEBS15 and MSAK16 of *Ceratocystis fimbriata*.

	Variables							
	AUURLLPC		AUDRLLPC		AURFCPC		AUWLPC	
Cultivars	CEBS15	MSAK16	CEBS15	MSAK16	CEBS15	MSAK16	CEBS15	MSAK16
Espada	569.6 aA	591.9 aA	228.3 aA	214.2 abA	1021.1 bA	938.9 aB	209.8 bB	313.1 aA
Haden	489.1 aA	567.4 aA	220.9 aA	243.7 aA	875.0 bcB	1008.9 aA	114.1 cB	207.2 bA
Palmer	488.7 aA	227.9 bB	227.1 aA	168.0 bB	1246.0 aA	992.3 aB	450.7 aA	0.0 cB
Tommy	306.7 bA	300.1 bA	185.1 aA	190.3 abA	866.2 bcB	973.9 aA	4.4 dA	0.0 cB
Ubá	244.1 bA	86.6 cB	204.5 aA	94.1 cB	805.0 cA	317.6 bB	0.0 eA	0.0 cA

For each variable, means within a column followed by the same lowercase letter or means within a row followed by the same uppercase letter are not significantly different ($P \leq 0.05$) as determined by Tukey' test.

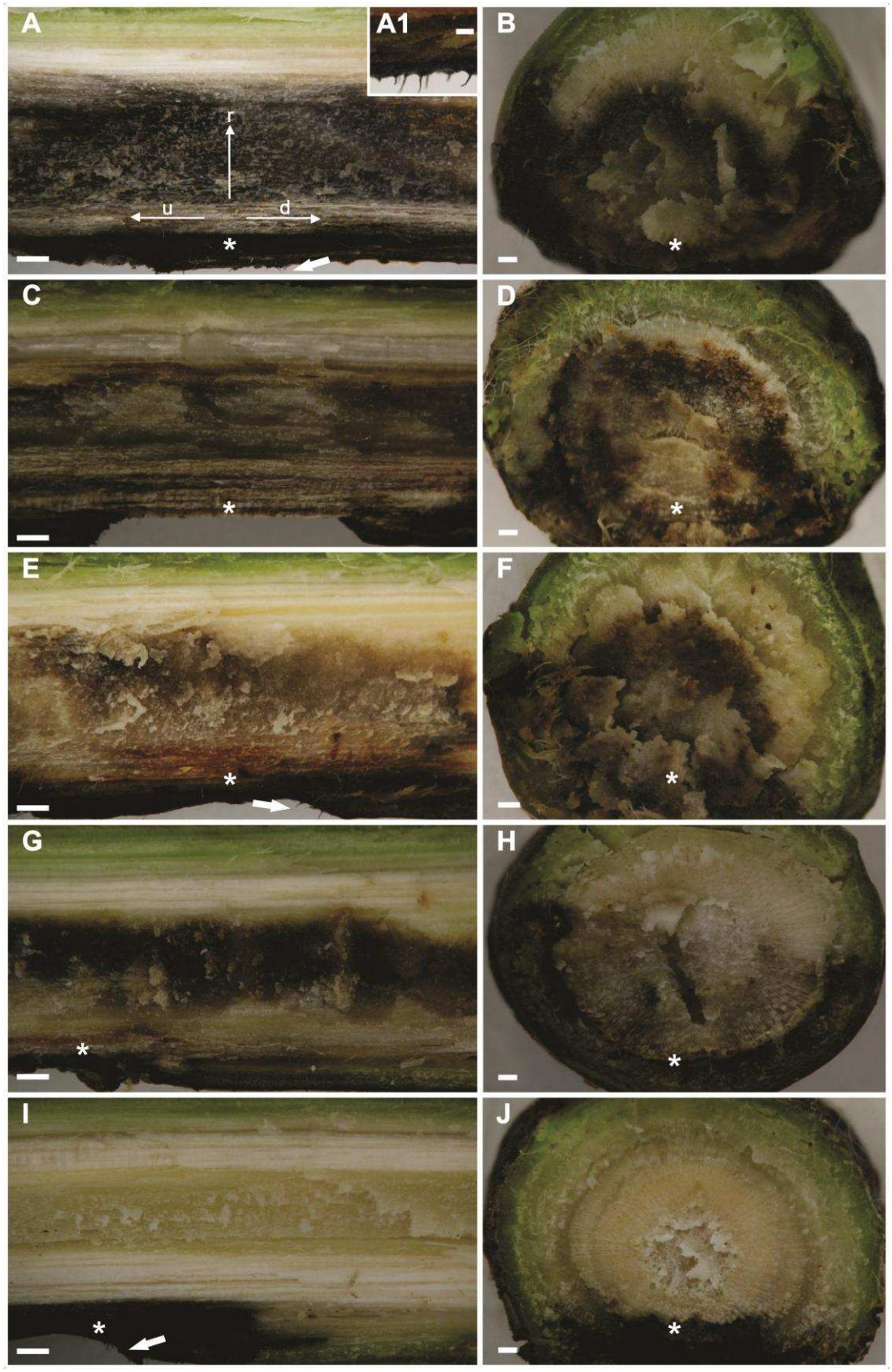

Figure 1

Figure 1 Symptoms of internal necrotic tissues in longitudinal (A, C, E, G and I) and transverse (B, D, F, H and J) stem sections from cultivars Espada (A and B), Haden (C and D), Palmer (E and F), Tommy Atkins (G and H) and Ubá (I and J) at 22 days after inoculation (dai) with the isolate MSAK16. Asterisks (*) indicate the stem region where the fungal inoculation occurred and from which the upward (u), downward (d) and radial (r) *Ceratocystis fimbriata* colonization were observed as detailed in A. The formation of perithecia of *C. fimbriata* was observed at the inoculation point of the stem tissues at 22 dai (arrow in A, E and I). In A1, perithecia of *C. fimbriata* are shown in a higher magnification. Scale bars: 1000 µm (A, B, C, D, E, F, G, H, I and J) and 500 µm (A1).

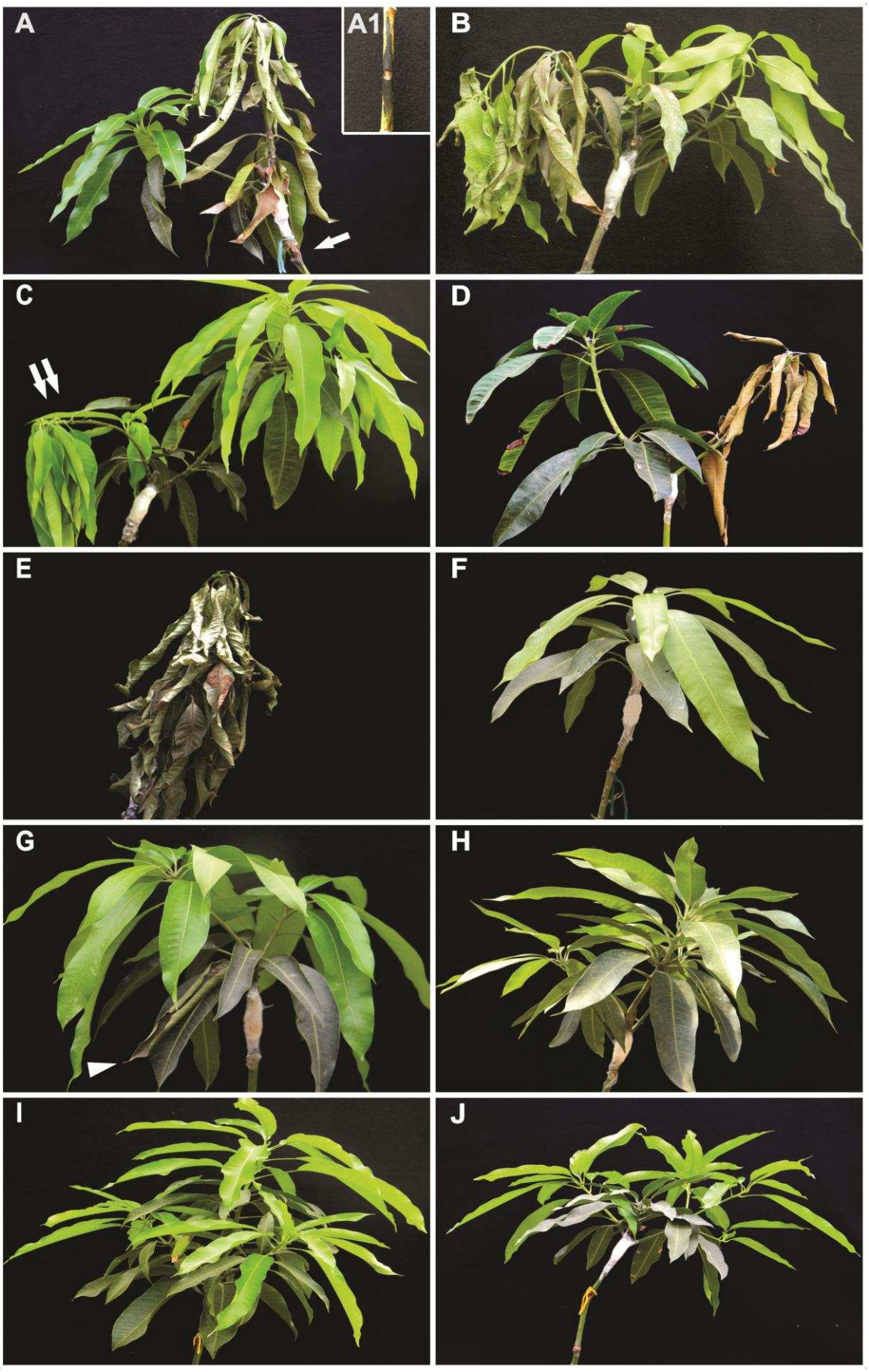

Figure 2

Figure 2 Symptoms of wilting in mango plants from cultivars Espada (A and B), Haden (C and D), Palmer (E and F), Tommy Atkins (G and H) and Ubá (I and J) at 22 days after inoculation with isolates CEBS15 (A, C, E, G and I) and MSAK16 (B, D, F, H and J) of *Ceratocystis fimbriata*. The arrow in A indicates symptoms of external necrotic stem tissue, which are detailed in A1. Double arrows in C indicate intense wilting without leaf blight, whereas the arrowhead in G shows symptoms in an early stage.

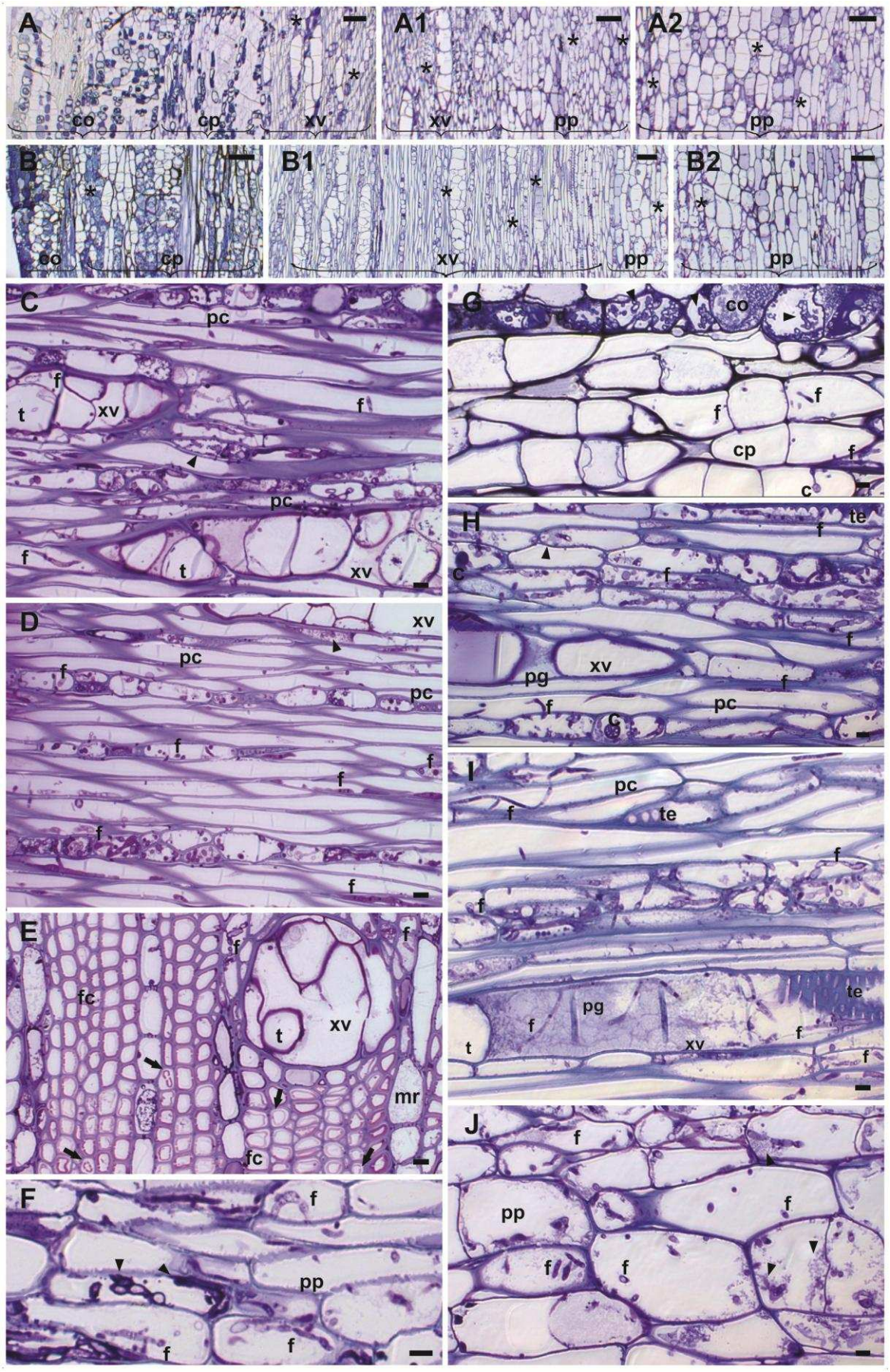
A
co
cp
xv
A1
xv
pp
A2
pp
B
co
cp
B1
xv
pp
B2
pp
C
pc
f
t
xv
f
pc
f
t
xv
D
xv
pc
f
pc
f
f
f
f
E
f
f
fc
t
xv
mr
fc
F
f
pp
f
f
G
co
f
f
cp
f
c
H
te
f
c
f
f
pg
xv
f
f
pc
c
I
pc
f
te
f
f
pg
te
f
f
t
xv
f
f
J
f
pp
f
f
f
f

Figure 3

Figure 3 Light micrographs of longitudinal (A, B, C, D, F, G, H, I and J) and transverse (E) mango stem tissues of the susceptible cultivar Espada at 22 days after inoculation with isolates CEBS15 (A, C, D, E and F) and MSAK16 (B, G, H, I and J). **A** and **B**, Sequential images of stem tissues colonized by *Ceratocystis fimbriata* (asterisks) starting from the collenchyma and then moving in the direction of the cortical parenchyma, xylem vessels and pith parenchyma. **C**, Hyphae of *C. fimbriata* (isolate CEBS15) grew abundantly in the parenchyma cells between xylem vessels. In some cells, amorphous granular material (arrowheads) was occasionally deposited around fungal hyphae. The fungus reached the xylem vessels, stimulating tylosis formation. **D**, In some parenchyma cells, fungal hyphae were thick. **E**, Hyphae of *C. fimbriata* colonized cells of the medullary radius and adjacent cells. Plasmatic membranes of some fiber cells, not yet colonized by the fungus, were detached, indicating possible cell death (arrows). Some xylem vessels were colonized by *C. fimbriata* with concomitant tylosis formation. **F**, Hyphae of *C. fimbriata* colonized the pith parenchyma in the radial direction. Some cells reacted to fungal invasion by accumulating amorphous granular material (arrowheads), indicating the presence of phenolic compounds. **G**, Hyphae of *C. fimbriata* (isolate MSAK16) in the collenchyma were often surrounded by amorphous granular material (arrowheads), whereas cortical parenchyma cells did not show any sign of reaction against fungal infection. Chlamydospores (aleurioconidia) were observed in the cortical parenchyma. **H**, Hyphae of *C. fimbriata* abundantly colonized the parenchyma cells with scarce deposition of amorphous granular material (arrowheads) around fungal hyphae. In some parenchyma cells, chlamydospores were observed and fungal hyphae were thick. Xylem vessels were obstructed by deposition of polysaccharide gel. **I**, Fungal hyphae grew abundantly in the parenchyma cells and the xylem vessels. Xylem vessels were obstructed by intense deposition of polysaccharide gels, fungal hyphae and tyloses. **J,** Some fungal hyphae in the pith parenchyma were surrounded by the amorphous granular material (arrowheads). Chlamydospores (c), collenchyma (co), cortical parenchyma (cp), fiber cells (fc), fungal hyphae (f), medullary radius (mr), parenchyma cells (pc), pith parenchyma (pp), polysaccharide gels (pg), tracheal elements (te), tylosis (t) and xylem vessels (xv). Scale bars: 100 µm (A and B) and 10 µm (C, D, E, F, G, H, I and J).

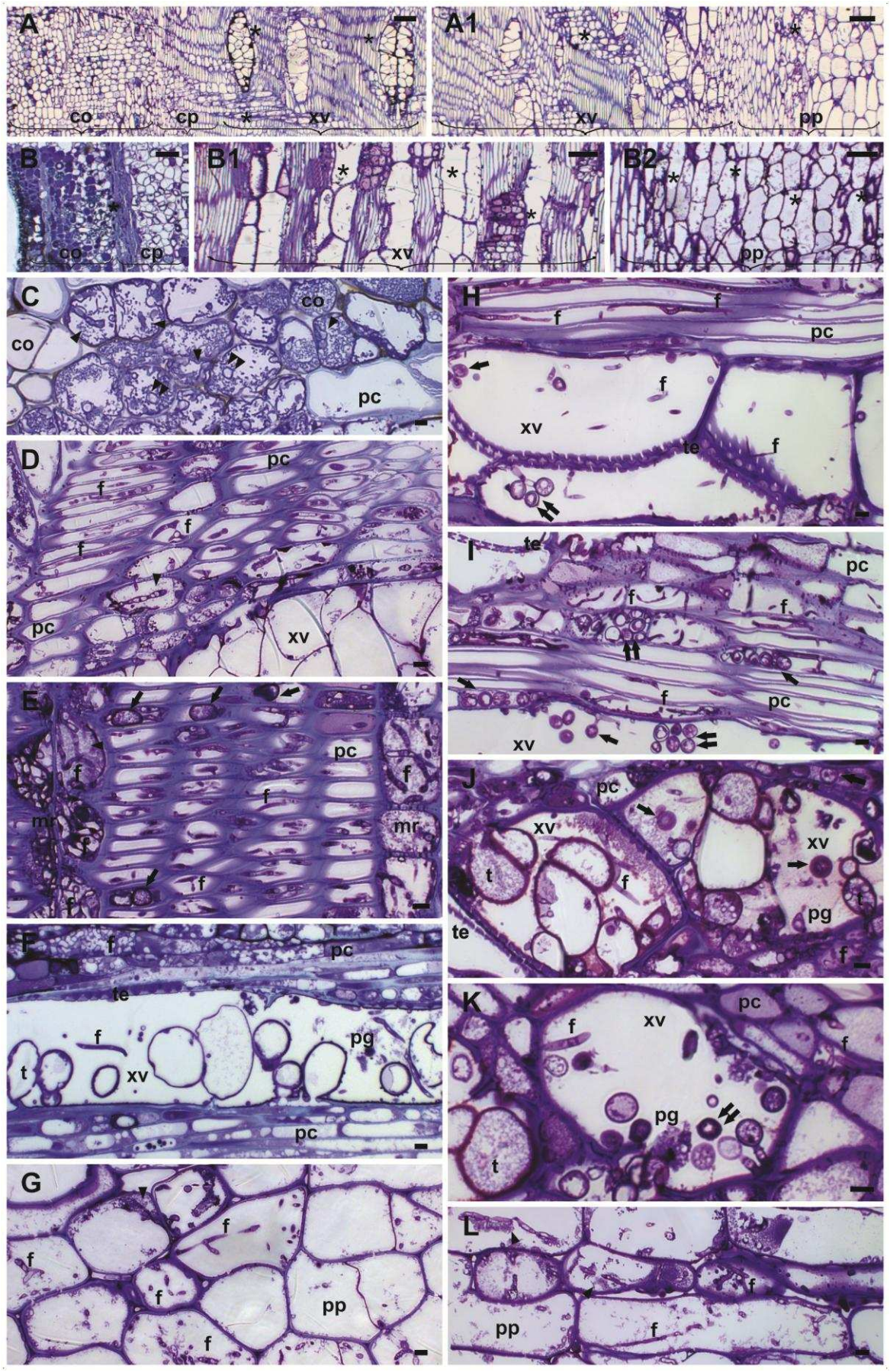
A
co
cp
xv
A1
xv
pp
B
co
cp
B1
xv
B2
pp
C
co
co
pc
D
pc
f
pc
xv
E
pc
f
mr
mr
F
f
pc
te
f
pg
t
xv
pc
G
f
pp
H
f
pc
f
xv
te
f
I
te
pc
f
f
pc
xv
J
pc
xv
xv
t
f
pg
te
K
pc
f
xv
f
pg
t
L
f
pp
f

Figure 4

Figure 4 Light micrographs of longitudinal (B, C, F, H, I and L) and transverse (A, D, E, G, J and K) mango stem tissues of the susceptible cultivar Haden at 22 days after inoculation with isolates CEBS15 (A, C, D, E, F and G) and MSAK16 (B, H, I, J, K and L). **A** and **B**, Sequential images of stem tissues colonized by *Ceratocystis fimbriata* (asterisks) starting from the collenchyma and then moving in the direction of the cortical parenchyma, xylem vessels and pith parenchyma. **C**, Hyphae of *C. fimbriata* (isolate CEBS15) in the collenchyma were often surrounded by amorphous granular material (arrowheads). In some cells, fungal hyphae appeared as empty shells (double arrowheads). **D**, Hyphae of *C. fimbriata* grew abundantly in the parenchyma cells adjacent to the xylem tissues. In some cells, amorphous granular material (arrowheads) was occasionally deposited around fungal hyphae. Large tylosis formation occurred in the xylem vessels. **E,** Fungal hyphae colonized cells of the medullary radius and parenchyma cells. In some parenchyma cells, large chlamydospores (aleurioconidia) were observed (arrow). **F,** Fungal hyphae grew abundantly in the parenchyma cells and xylem vessels. Xylem vessels were obstructed by the deposition of polysaccharide gels, fungal hyphae and tylosis. **G,** Hyphae of *C. fimbriata* apparently massively colonized the pith parenchyma in the radial direction. Some cells reacted to fungal invasion by accumulating amorphous granular material (arrowheads). **H and I,** Hyphae of *C. fimbriata* (isolate MSAK16) colonized the parenchyma cells and the xylem vessels. Many chlamydospores were observed (arrow) in the parenchyma cells and xylem vessels and some of them seemed to be been formed in chains (double arrow). **J and K,** Xylem vessels were obstructed by intense deposition of polysaccharide gels, fungal hyphae, chlamydospores (arrow) and large tyloses. Chlamydospores in chains were also noted (double arrow). Some tylosis stained dark-blue or purple, indicating the presence of phenolic compounds. **L,** Some fungal hyphae in the pith parenchyma were surrounded by the amorphous granular material (arrowheads). Collenchyma (co), cortical parenchyma (cp), fungal hyphae (f), medullary radius (mr), parenchyma cells (pc), pith parenchyma (pp), polysaccharide gels (pg), tracheal elements (te), tylosis (t) and xylem vessels (xv). Scale bars: 100 µm (A and B) and 10 µm (C, D, E, F, G, H, I, J, K and L).

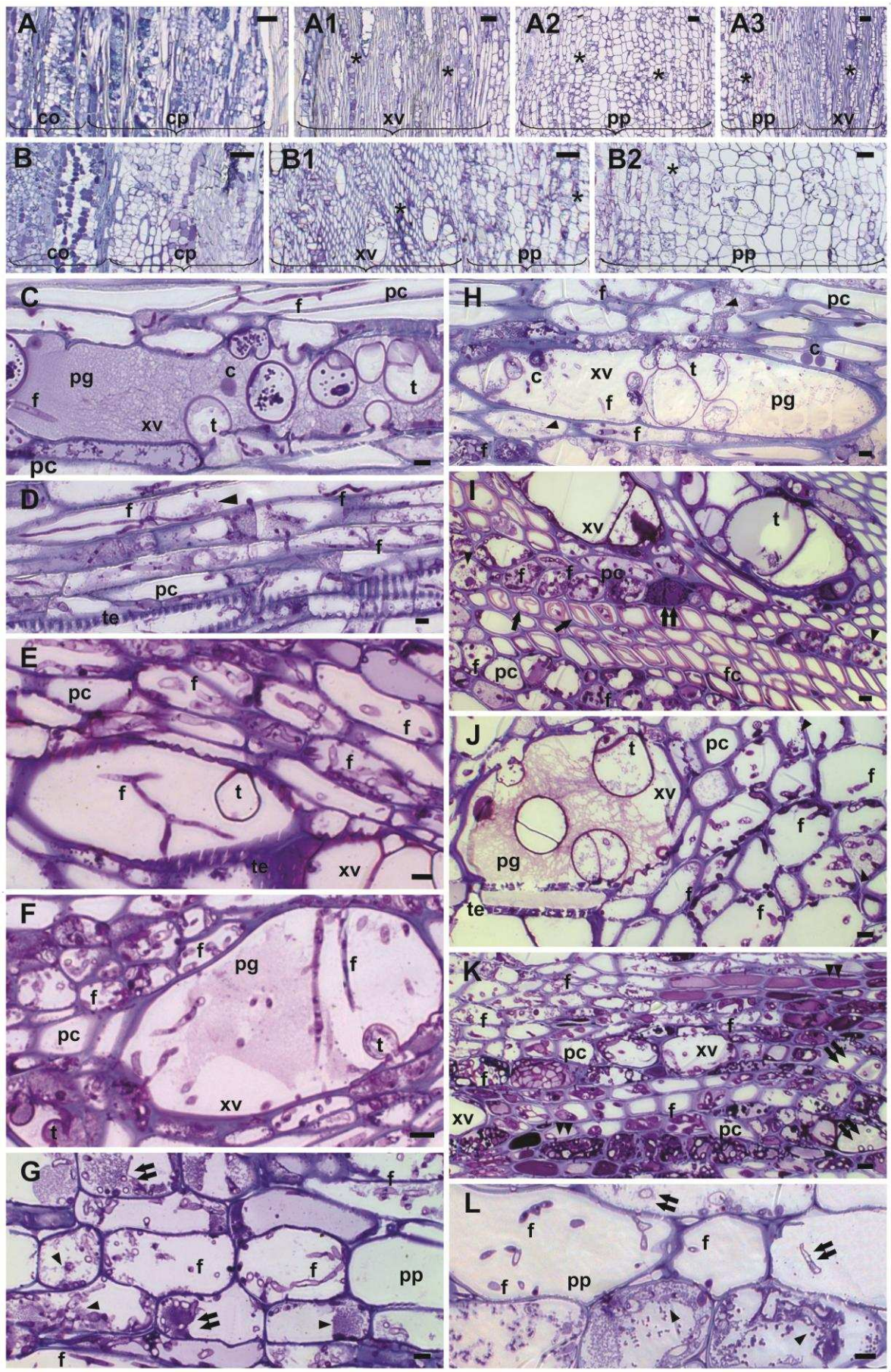
A
co
cp
A1
xv
A2
pp
A3
pp
xv
B
co
cp
B1
xv
pp
B2
pp
C
pc
f
pg
c
t
f
xv
t
pc
D
f
f
f
pc
te
E
pc
f
f
f
f
t
te
xv
F
f
pg
f
f
pc
t
xv
t
G
f
f
f
f
pp
f
H
f
pc
c
c
xv
t
f
pg
f
f
I
xv
t
f
f
pc
f
pc
fc
J
t
pc
xv
f
f
pg
te
f
f
K
f
f
f
pc
xv
f
xv
f
pc
L
f
f
f
pp

Figure 5

Figure 5 Light micrographs of longitudinal (A, C, D and G) and transverse (B, E, F, H, I, J, K and L) mango stem tissues of the susceptible cultivar Palmer at 22 days after inoculation with isolates CEBS15 (A, C, D, E, F and G) and MSAK16 (B, H, I, J, K and L). **A** and **B**, Sequential images of stem tissues colonized by *Ceratocystis fimbriata* (asterisks) starting from the collenchyma and then moving in the direction of the cortical parenchyma, xylem vessels and pith parenchyma. **C,** Xylem vessels were obstructed by intense deposition of polysaccharide gels, fungal hyphae, chlamydospores (aleurioconidia) and tyloses. **D,** Long hyphae of *C. fimbriata* (isolate CEBS15) grew in the parenchyma cells adjacent to the tracheal elements. Amorphous granular material (arrowheads) was scarcely deposited around fungal hyphae. **E and F,** Fungal hyphae grew abundantly in the parenchyma cells and the xylem vessels. Xylem vessels were obstructed by deposition of polysaccharide gels, long and thickened fungal hyphae and tyloses. Some tyloses stained dark-blue or purple. **G,** Hyphae of *C. fimbriata* apparently colonized all pith parenchyma in the radial direction and reached the xylem vessels. Some cells reacted to fungal invasion by accumulating amorphous granular material (arrowheads) and sometimes, fungal hyphae appeared as empty shells (double arrow). **H,** Hyphae of *C. fimbriata* (isolate MSAK16) grew abundantly in the parenchyma cells and xylem vessels. Chlamydospores were also observed. Amorphous granular material (arrowheads) was scarcely deposited around fungal hyphae. Xylem vessels were obstructed by deposition of polysaccharide gels, fungal hyphae, chlamydospores and tyloses. **I,** Hyphae of *C. fimbriata* colonized the parenchyma cells between the xylem vessels. Xylem vessels were obstructed by intense tylosis formation. Plasmatic membranes of some fiber cells, not yet colonized by the fungus, were detached, indicating possible cell death (arrows). Others parenchyma cells reacted to fungal invasion by accumulating amorphous granular material (arrowheads) around fungal hyphae or were stained as dark-blue or purple (double arrowheads), indicating the presence of phenolic compounds. **J,** Xylem vessels were obstructed by intense deposition of polysaccharide gels, fungal hyphae and tyloses. Some tyloses stained dark-blue or purple. **K,** Hyphae of *C. fimbriata* colonized the parenchyma cells adjacent to the xylem vessels. Some parenchyma cells reacted to fungal invasion by accumulating amorphous material that stained dark-blue or purple (double arrowheads). Sometimes, fungal hyphae appeared as empty shells (double arrow). **L**, Some fungal hyphae in the pith parenchyma were surrounded by an amorphous granular material

(arrowheads) and sometimes appeared as empty shells (double arrow). Chlamydospores (c), collenchyma (co), cortical parenchyma (cp), fiber cells (fc), fungal hyphae (f), parenchyma cells (pc), pith parenchyma (pp), polysaccharide gels (pg), tracheal elements (te), tylosis (t) and xylem vessels (xv). Scale bars: 100 µm (A and B) and 10 µm (C, D, E, F, G, H, I, J, K and L).

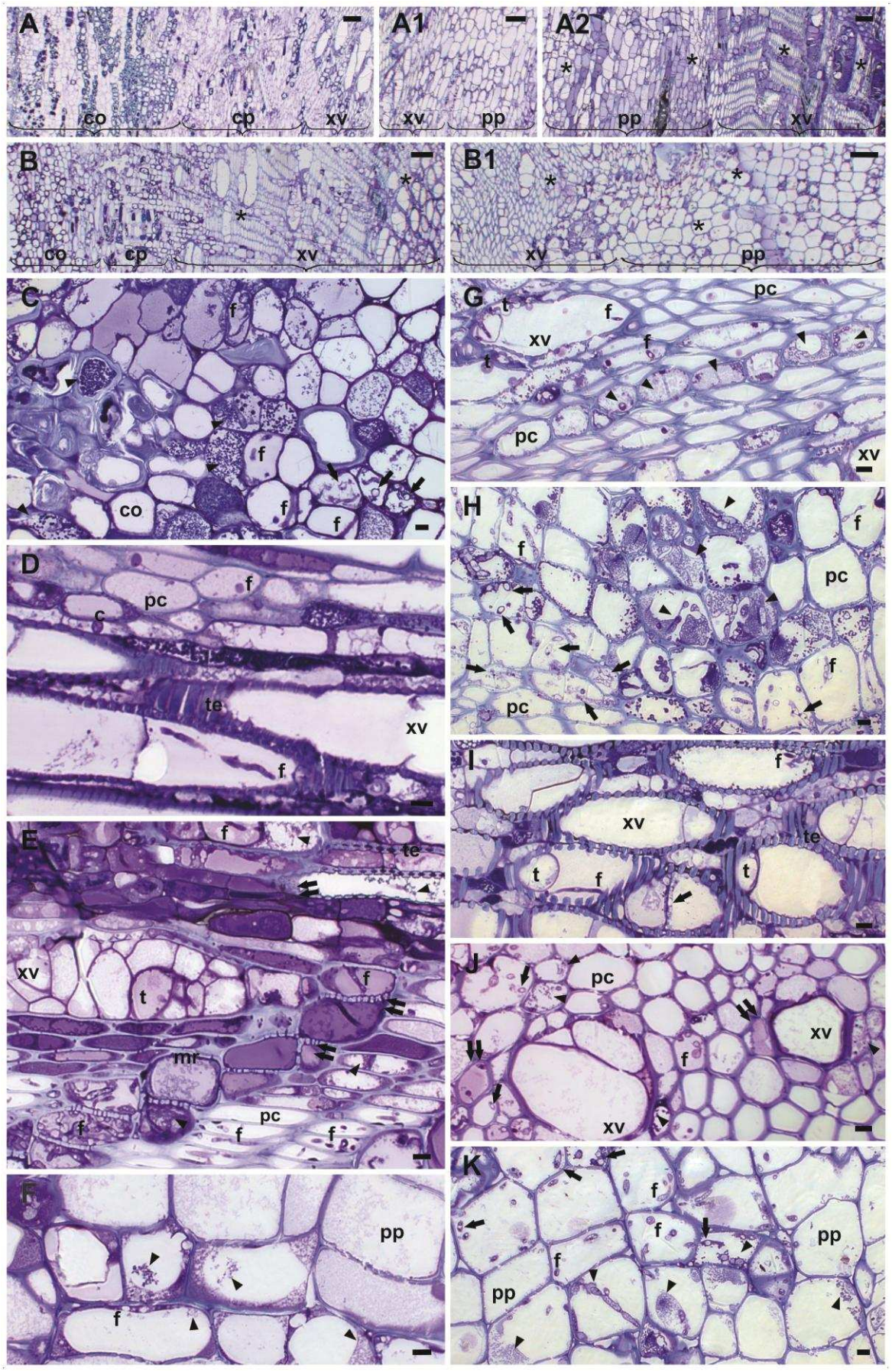
A
co
cp
xv
A1
xv
pp
A2
pp
xv
B
co
cp
xv
B1
xv
pp
C
co
f
D
pc
c
te
xv
f
E
te
xv
t
mr
pc
F
pp
G
t
xv
pc
H
pc
I
xv
te
J
pc
xv
K
pp

Figure 6

Figure 6 Light micrographs of longitudinal (A, D, E and F) and transverse (B, C, G, H, I, J and K) mango stem tissues of the moderately resistant cultivar Tommy Atkins at 22 days after inoculation with isolates CEBS15 (A, C, D, E, F) and MSAK16 (B, G, H, I, J, K). **A** and **B**, Sequential images of stem tissues colonized by *Ceratocystis fimbriata* (asterisks) starting from the collenchyma and then moving in the direction of the cortical parenchyma, xylem vessels and pith parenchyma. **C**, Hyphae of *C. fimbriata* (isolate CEBS15) in the collenchyma were scarce and surrounded by amorphous granular material (arrowheads). In some cells, fungal hyphae appeared as empty shells (arrow), whereas others were thin and faint. **D,** Hyphae and chlamydospores (aleurioconidia) of *C. fimbriata* occasionally grew in the parenchyma cells and xylem vessels. Xylems vessels were free of any occlusions, although faint fungal hyphae were observed in some of them. **E,** Most of the parenchyma and medullary radius cells colonized by *C. fimbriata* reacted to fungal infection by the deposition of amorphous granular material (arrowheads) around fungal hyphae or were stained dark-blue or purple (double arrow). The xylem vessels were obstructed by large tyloses that stained dark-blue or purple, indicating the presence of phenolic compounds. **F,** Hyphae of *C. fimbriata* scarcely colonized the pith parenchyma in the radial direction. Most of the cells reacted to fungal invasion by accumulating amorphous granular material (arrowheads). **G,** Hyphae of *C. fimbriata* (isolate MSAK16) occasionally colonized the parenchyma cells and the xylem vessels. In the parenchyma cells, amorphous granular material occurred frequently around fungal hyphae, whereas in the xylem vessels, fungal hyphae were faint and the vessels were free of polysaccharides gels, but contained small tyloses that stained dark-blue or purple. **H,** Parenchyma cells adjacent to the xylem vessels showed intense deposition of amorphous granular material around the fungal hyphae (arrowheads). Frequently, fungal hyphae appeared as empty shells (arrow) or were thin and faint. **I,** In the xylem vessels, fungal hyphae were faint or appeared as empty shells (arrow) and the vessels were frequently free of large obstructions. **J,** Most of the parenchyma cells adjacent to the xylem vessels infected by *C. fimbriata* stained dark-blue or purple (double arrow) or accumulated amorphous granular material (arrowheads) around fungal hyphae. Some hyphae of *C. fimbriata* appeared as empty shells (arrow) and the xylem vessels were free of any occlusions. **K,** Most of the fungal hyphae in the pith parenchyma were surrounded by amorphous granular material (arrowheads) and sometimes appeared as empty shells (arrow).

Chlamydospores (c), collenchyma (co), cortical parenchyma (cp), fungal hyphae (f), medullary radius (mr), parenchyma cells (pc), pith parenchyma (pp), tracheal elements (te), tylosis (t) and xylem vessels (xv). Scale bars: 100 µm (A and B) and 10 µm (C, D, E, F, G, H, I, J and K).

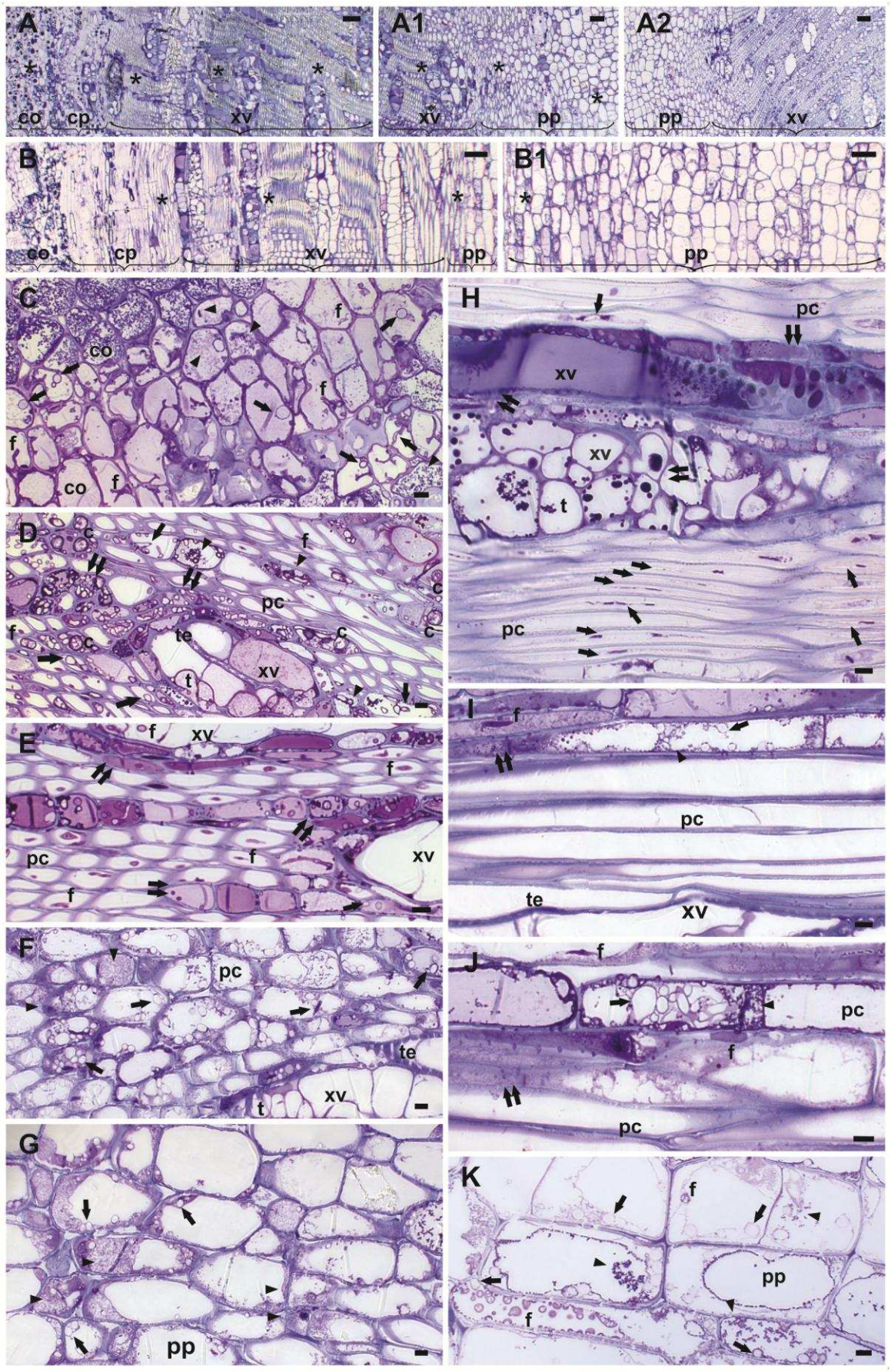
A
co
cp
xv
A1
xv
pp
A2
pp
xv
B
co
cp
xv
pp
B1
pp
C
co
f
co
f
D
c
pc
te
t
xv
E
f
xv
pc
F
pc
te
t
xv
G
pp
H
pc
xv
t
pc
I
f
pc
te
xv
J
f
pc
pc
K
f
pp
f

Figure 7

Figure 7 Light micrographs of longitudinal (B, H, I, J and K) and transverse (A, C, D, E, F and G) mango stem tissues of the resistant cultivar Ubá at 22 days after inoculation with isolates CEBS15 (A, C, D, E, F and G) and MSAK16 (B, H, I, J and K). **A** and **B**, Sequential images of stem tissues colonized by *Ceratocystis fimbriata* (asterisks) starting from the collenchyma and then moving in the direction of the cortical parenchyma, xylem vessels and pith parenchyma. **C**, Hyphae of *C. fimbriata* (isolate CEBS15) in the collenchyma were scarce and surrounded by amorphous granular material (arrowheads). In some cells, fungal hyphae appeared as empty shells (arrow), whereas others were thin and faint. **D**, Most of the parenchyma cells colonized by *C. fimbriata* reacted strongly to fungal invasion and many hyphae appear as empty shells (arrow). Some cells stained dark-blue or purple (double arrow), whereas others accumulated amorphous granular material around fungal hyphae (arrowheads). In some parenchyma cells, chlamydospores (aleurioconidia) were observed. In the xylem vessels, fungal hyphae were faint and the vessels were free of polysaccharides gels but contained tyloses that stained dark-blue or purple, indicating the presence of phenolic compounds. **E,** Many parenchyma cells adjacent to the xylem vessels reacted strongly to fungal invasion and stained dark-blue or purple (double arrow). Xylems were free of any occlusions, although some vessels contained hyphae of *C. fimbriata.* **F,** Many parenchyma cells colonized by *C. fimbriata* accumulated amorphous granular material around fungal hyphae (arrowheads) and most of the hyphae appeared as empty shells (arrow). Tyloses were observed in the xylem vessels. **G,** Hyphae of *C. fimbriata* occasionally colonized the pith parenchyma in the radial direction. Many cells reacted to fungal invasion by accumulating amorphous granular material (arrowheads) and most hyphae appeared as empty shells (arrow). **H,** Most hyphae of *C. fimbriata* (isolate MSAK16) colonizing the parenchyma cells appeared as empty shells (arrow), whereas others were thin and faint. Xylem vessels stained as dark-blue or purple (double arrow), indicating the presence of phenolic compounds. They also contained many tyloses. **I and J,** Fungal hyphae scarcely grew in the parenchyma cells adjacent to the xylem vessels, which reacted to fungal infection through the deposition of amorphous granular material (arrowheads) around the pathogen or the cell were stained dark-blue or purple (double arrow). Many hyphae of *C. fimbriata* appeared as empty shells (arrow). Xylem vessels were free of any occlusions. **K,** Many fungal hyphae in the pith parenchyma were surrounded by amorphous granular material (arrowheads) and

appeared as empty shells (arrow) or were faint. Plasmatic membranes of some pith parenchyma cells were detached, indicating possible cell death. Collenchyma (co), cortical parenchyma (cp), fungal hyphae (f), parenchyma cells (pc), pith parenchyma (pp), tracheal elements (te), tylosis (t) and xylem vessels (xv). Scale bars: 100 µm (A and B) and 10 µm (C, D, E, F, G, H, I, J and K).

CHAPTER 2

Accepted as original paper to *Phytopathology*

Resistance in Mango Against Infection by *Ceratocystis fimbriata*

Leonardo Araujo, Wilka Messner Silva Bispo, Isaías Severino Cacique, Wiler Ribas Moreira and Fabrício Ávila Rodrigues

Viçosa Federal University, Department of Plant Pathology, Laboratory of Host-Pathogen Interaction, Viçosa, Minas Gerais State, Zip Code 36570-900, Brazil

ABSTRACT

Araujo, L., Bispo, W. M. S., Cacique, I. S., Moreira, W. R., and Rodrigues, F. A. Resistance in mango against infection by *Ceratocystis fimbriata*. Phytopathology 104:xx-xx.

This study was designed to characterize and describe host cell responses of stem tissue to mango wilt disease caused by the fungus *Ceratocystis fimbriata* in Brazil. Disease progress was followed, through time, in inoculated stems for two cultivars, Ubá (field resistant) and Haden (field susceptible). Stem sections from inoculated areas were examined using fluorescence light microscopy, transmission and scanning electron microscopy coupled with energy dispersive X-ray microanalysis. Tissue from Ubá colonized by *C. fimbriata* had stronger autofluorescence than those from Haden. The X-ray microanalysis revealed that the tissue of Ubá had higher levels of insoluble sulfur and calcium than those of the Haden. Scanning electron microscopy revealed that fungal hyphae, chlamydospores (aleurioconidia) and perithecia-like structures of *C. fimbriata* were more abundant in Haden relative to Ubá. At the ultrastructural level, pathogen hyphae had grown into the degraded walls of parenchyma, fiber cells and xylem vessels in the tissue of Haden. However, in Ubá, plant cell walls were rarely degraded and hyphae were often surrounded by dense amorphous granular materials and hyphae appeared to have died. Taken together, the results of study characterize the susceptible and resistant basal cell responses of mango stem tissue to infection by *C. fimbriata.*

Additional keywords: calcium, barrier zones, mango wilt, phenolic-like compounds, sulfur, vascular pathogen.

INTRODUCTION

Worldwide mango (*Mangifera indica* L.) is one of the most important tropical fruit crops (22). The adaptability of mango cultivars to different environmental conditions and their resistance to multiple diseases are among the factors that greatly improve mango quality and yield (12). Mango wilt is caused by *Ceratocystis fimbriata* Ellis & Halst. (23,56) in Brazil (41), while a similar wilt disease is found in Oman and Pakistan, where it is attributed to *C. manginecans* (1,55). Thus, mango wilt has become a serious concern to growers (1,55). *Ceratocystis fimbriata* causes death of the entire tree either a few months after the fungus penetrates the roots, or more slowly if it enters through wounded branches of the canopy (41). Typical disease symptoms include wilting and browning of leaves on single branches and gum exudation from the trunks (41,56). As the infection progresses, the internal and external stem tissue becomes dark brown due to intensive necrosis (41,56).

The eradication of mango trees with wilt symptoms can be used as a strategy to slow disease progress (41,46). However, in Brazil, mango cultivars with high levels of resistance to mango wilt are the most effective strategy adopted by farmers to control the disease (12,40,41,46). Resistance is critical since mango wilt cannot be controlled by fungicides (12,40,41,46). The high degree of genetic variability in aggressiveness of *C. fimbriata* renders, resistant mango cultivars to become susceptible in a relatively short time (40,41,46).

The resistance of trees to vascular pathogens is primarily based on their ability to restrict pathogen infection to a few cells (20). Suberized bark containing phenolic-like compounds, the composition of the xylem vessels and their diameter are common examples of pre-formed mechanisms that restrict infection by vascular pathogens (6,20,32). In contrast, active defense mechanisms include anatomical responses, like deposition of gels and the formation of tyloses in invaded vascular vessels (9,20). The formation of barrier zones, intense lignification and suberization of cell walls, and the production of phenolics, phytoalexins and proteins related to pathogenesis are also involved in active defenses (9,20,43).

Pre- or post- infection phenolics play a pivotal role in the host defense against pathogenic infection (34), primarily because of their effect on cell wall lignification (5), antimicrobial activity (45), modulation of plant hormones involved in defense signaling pathways and in the scavenging of reactive oxygen species (19). Suberin,

phytoalexins, phenolics and lignin are the major components in barrier zones formed in host tissue in response to pathogen infection (9,11,43,49,53).

Important insights into specific responses in infected tissue to pathogen infection can be obtained by examining autofluorescence (2,9,21,29,43). Autofluorescence can be used because phenolics and related polymers like lignin absorb short wave length light, in ultraviolet (UV) and near-blue range, and emit longer wavelengths of visible light (2,9,21,29,43). Thus, microscopes capable of producing UV and near-blue light for excitation of phenolics and fitted with the proper filters will readily reveal localized autofluorescent compounds in tissue (2,9,21,29,43). For example, stem sections from balsam poplar infected by *Ophiostoma novo-ulmi* when observed under UV light excitation showed stronger autofluorescence in cellular barrier zones (43). Intense autofluorescence was also produced by suberin and lignin in callus cultures of American elm infected by *O. novo-ulmi* (2). Eynck et al. (21) observed intense deposition of phenolics and lignin compounds in the roots and hypocotyls of plants from a resistant cultivar of oilseed rape in response to infection by *Verticillium longisporum*, when compared to tissue from plants of a susceptible cultivar. The resistant cultivar exhibited a much stronger autofluorescence when excited by light in the near-UV range than the susceptible cultivar (21).

The concentration of certain chemical elements in plant tissue also can affect their resistance to vascular pathogens (17). High levels of sulfur in stem tissue of cacao (15) and tomato (57) plants were associated with increased resistance to infection by *V. dahliae.* Sulfur and sulfur compounds also decrease disease directly as a result of antimicrobial activities and indirectly by enhancing host resistance (27). Increased calcium content in plant tissue also correlates with the resistance of cell walls and the middle lamella to fungal pathogen invasion (3,13,39). Calcium also acts as a signal for oxidative bursts that trigger the synthesis of phytoalexins and the induction of defense-related genes whose products lead to resistance in many host-pathogen interactions (30,39).

The presence of amorphous material is a typical feature of active plant cell defense of against infection by pathogenic fungi (4,5,21,26,45). Amorphous material is frequently associated with phenolic-like compounds because of its texture, osmiophilic properties (47) and ability to alter fungal hyphae (7,8,35,44,45). According to Hall et al. (26), accumulation of amorphous materials identified as terpenoid phytoalexins in the xylem vessels and adjacent parenchyma cells in the

roots of a resistant cotton cultivar restricted the colonization of *Fusarium oxysporum* f.sp. *vasinfectum.*

The objectives of the current study were to describe and characterize host responses to *C. fimbriata* in stems of resistant and susceptible mango cultivars with a view of discovering more effective ways to control mango wilt. To achieve these objectives, an infection time course in two mango cultivars, Ubá (resistant) and Haden (susceptible) was employed. Both fluorescence light microscopy, and transmission and scanning electron microscopy coupled with energy dispersive X-ray microanalysis were used to help describe and characterize cellular responses in stem tissue of two cultivars.

MATERIALS AND METHODS

Plant material. Mango plant cultivars Haden (susceptible) and Ubá (resistant) were obtained from a commercial nursery (Dona Euzébia city, Minas Gerais State, Brazil) and their rootstock was from the cv. Imbú. The 1.5-year-old plants were transplanted into plastic pots containing 8 kg of soil, sand and manure in a 2:1:1 proportion. Plants were kept in a greenhouse (temperature of 30 ± 2°C during day and 10°C at night and relative humidity of 70 ± 5%) for 2 months before starting the experiments.

Inoculation procedure. The isolate MSAK16 of *C. fimbriata* used to inoculate the plants was obtained from symptomatic mango plants collected in Aquidauana, Mato Grosso do Sul State, Brazil. The isolate was preserved using Castellani's method (18). Plugs of a malt extract agar medium containing fungal mycelia were transferred to Petri dishes containing potato dextrose agar (PDA). After three days, the PDA plugs containing fungal mycelia were transferred to Petri dishes containing the same culture medium and maintained in an incubator (temperature of 25°C and 12 h photoperiod) for 14 days.

Inoculation was performed following the methods of Al-Sadi et al. (1). Bark disks (10-mm diameter and 2-mm height) were removed from the stems of both cultivars using a punch. The disks came from approximately 5 cm above the graft scar. A plug (10-mm diameter) removed from the middle portion of each PDA plate obtained from 14-day-old colonies of *C. fimbriata* was placed in the wound. Each wound containing the fungal mycelia PDA plug was carefully covered with a piece of moistened cotton and enclosed with parafilm to maintain adequate moisture to promote fungal infection. Wounds only receiving plugs of PDA medium served as the control.

Disease assessment. Disease progress in stem tissue and development of wilted leaves was evaluated at 15, 22 and 29 days after inoculation (dai). The upward, downward and radial colonization of the stem tissue by the hyphae of *C. fimbriata* was accomplished by measuring the length (in cm) of internal necrotic tissue using an electronic digital caliper (Neiko 01407A, Stainless Steel, Mandaluyong, Philippines). Upward relative lesion length (URLL) and downward relative lesion length (DRLL) were expressed as the ratio between the length from the graft scar to the top of the stem (LGST) and the lesion length (LL) taken from the same area (upward and downward) beginning at the inoculation point. The following formula:

URLL or DRLL = LL × 100/LGST was used. The stem of each plant was standardized to a length of 20 cm (distance from the graft scar to the top of the stem). The radial fungal colonization (RFC) was determined as the length of the necrotic tissue in relation to the total stem diameter × 100. Symptoms of internal necrotic tissue in both longitudinal and transverse stem sections inoculated with *C. fimbriata* were photographed at 6.5 X for whole stem tissue and at 40 X for stem tissue-associated perithecia. This was done using a stereomicroscope (Stemi 2000-C, Carl Zeiss, Germany) coupled to a digital camera (PowerShot A640, Canon).

The percentage of wilted leaves from the total number of leaves per plant of each cultivar was determined using the methods of Al-Sadi et al. (1). Representative mango plants infected with *C. fimbriata* were digitally photographed (Coolpix L110, Nikon) at each sampling time to record the pattern of wilting development.

Data from URLL, DRLL, RFC and the percentage of wilted leaves were used to calculate the area under the upward relative lesion length progress curve (AUURLLPC), the area under the downward relative lesion length progress curve (AUDRLLPC), the area under the radial fungal colonization progress curve (AURFCPC) and the area under the wilted leaves progress curve (AUWLPC), respectively, according to the methods of Shaner and Finney (48).

Processing the infected stem tissue for microscopic studies. A total of 25 to 30 transverse and longitudinal stem sections from four plants of the two cultivars (10-mm thick) were obtained from 3 cm below and above the inoculation point at 15, 22 and 29 dai. Stem sections of non-inoculated plants served as comparative controls. Stem sections were carefully transferred to glass vials containing 10 ml of fixative composed of 3% (v/v) glutaraldehyde and 2% paraformaldehyde (v/v) in 0.1 M sodium cacodylate buffer (pH 7.2). Vials were then covered in aluminum foil and stored at 4°C for two months (45) until used for microscopic studies.

Fluorescence microscopy. A total of four transverse and longitudinal stem sections from inoculated plants of Haden and Ubá were washed three times with distilled water and mounted on glass slides with two drops of a glycerine:water solution (2:8, v/v) according to the basic methodology of Eynck et al. (21) and Koga et al. (29). Stem sections from non-inoculated plants of the two cultivars served as the control treatment.

Autofluorescence of stem sections was achieved using an fluorescent Carl Zeiss Axio Imager A1 microscope (Carl Zeiss, Germany) with Zeiss filter sets 01 (UV;

365 nm excitation, 395 nm beam splitter and 397 nm emission) and 05 (blue; 395-400 nm excitation, 460 nm beam splitter and 470 nm emission). Images were acquired digitally (Axio Cam HR, Carl Zeiss) and further processed with Axion Vision 4.8.1 software.

X-ray microanalysis. Insoluble elemental composition and relative levels in transverse stem tissue of Haden and Ubá collected at 22 and 29 dai were investigated by energy dispersive X-ray spectroscopy (EDS) using a scanning electron microscope (LEO 1430VP, Carl Zeiss, Jena, Thuringia, Germany) with an attached X-ray detector system (Tracor TN5502, Middleton, WI, USA). Samples were dehydrated in ethanol, submitted to critical point drying in CO_2 (Bal-tec, model CPD 030; Electron Microscopy Sciences (EMS), Hatfield, PA, USA). Specimens were mounted onto aluminum stubs (two specimens from each sample) and coated with a thin film of evaporated carbon (Quorum Q150 T, East Grinstead, West Sussex, England, UK). Because soluble (diffusible) elements are lost during liquid ethanol dehydration and substitution with liquid CO_2, the remaining element should be considered largely bound to cell components and therefore insoluble (58).

The EDS microanalysis on all specimens was performed at magnifications of 40 and 1000 X with an accelerating voltage of 20 kV and a working distance of 19 mm. For each treatment, a total area of 18×10^7 μm^2 was analyzed in each sample of stem tissue. The distribution patterns of calcium (Ca), iron (Fe), magnesium (Mg), manganese (Mn), potassium (K) and sulfur (S) were based on secondary electron images, X-ray emission spectra and corresponding X-ray elemental maps according to the methods of Goldstein et al. (24) and Williams et al. (57). A total of ten images were obtained from each sample of stem tissue per treatment.

Scanning electron microscopy. Transverse and longitudinal stem tissue from Haden and Ubá were collected at 22 and 29 dai, washed with sodium cacodylate buffer (0.1 M) and postfixed for 1 h at room temperature with 1% (w/v) osmium tetroxide prepared in the same buffer. Samples were dehydrated and mounted on aluminum stubs and sputter coated with gold (Balzers Union, model FDU 010; EMS, Hatfield, PA, USA). A LEO scanning electron microscope (SEM) operating at 10 Kv, with a working distance ranging from 10 to 30 mm (24,51), was used to obtain photomicrographs. For each treatment, two stubs with two samples of stem tissue were examined by SEM.

Transmission electron microscopy. Transverse and longitudinal stem tissue were collected at 22 dai and washed and postfixed with 1% (w/v) osmium tetroxide. Samples were then dehydrated and embedded in Spurr's resin (EMS, Hatfield, PA, USA) in a 25% and 33% gradient for 1 h, 66% and 75% gradient for 12 h and 100% resin for 36 h. Because of their extreme sample hardness, they were placed in a vacuum chamber for 3 min at each gradient to allow better resin infiltration. The samples were mounted in flat embedding molds and embedded in pure Spurr's resin and polymerized in an oven at 65°C for 24 h. Thick sections (0.5 µm) were cut from the embedded material with glass knives using a Leica RM 2245 rotary microtome (Leica Microsystems®, Nussloch, Germany). Sections were stained with 1% toluidine blue in 2% sodium borate for 5 min for light microscope observations. Once infection threads were located under the light microscope, ultrathin sections (70 nm) were taken from the embedded material using a diamond knife (Diatome, Hatfield, PA, USA) using a Power Tome-X ultramicrotome (RMC, Boeckeler Instruments, Tucson, AZ, USA). Ultrathin sections were mounted on copper grids (200 mesh square), stained with 2% uranyl acetate and 1% lead acetate for 20 min each and examined by transmission electron microscopy (TEM) (Zeiss EM 109, Carl-Zeiss, Oberkochen, Germany) operating at 80 Kv according to the methods of Bozzola and Russel (10) and Rodrigues et al. (45). For each treatment, four blocks were carefully selected for cuttings, and from each block ten thick and eight to sixteen ultrathin sections were examined under the light and transmission electron microscopes, respectively.

Experimental design and data analysis. For comparison of the two mango cultivars, a completely randomized design with four replications was used. Each replication consisted of a plastic plot containing one mango plant. The total experiment was repeated once. Data from AUURLLPC, AUDRLLPC, AURFCPC and AUWLPC were analyzed with analysis of variance (ANOVA) and the treatment means compared by an *F*-test ($P \leq 0.05$) using SAS (Release 8.02 Level 02M0 for Windows, SAS Institute, Inc., 1989, Cary, NC, USA).

RESULTS

Disease assessment. The AUURLLPC, AUDRLLPC, AURFCPC and AUWLPC were significantly higher for the susceptible Haden when compared to the resistant Ubá (Table 1). Plants from Haden started to wilt at 13 dai, whereas plants from Ubá did not wilt until the end of the experiments (Fig. 1). Stem tissue obtained from Haden had more internal necrosis than did the stem tissue of Ubá (Figs. 1; 2C, D, E, F, G, H; 3C, D, E, F, G and H).

Fluorescence microscopy. Stem sections from non-inoculated plants of each cultivar did not show autofluorescence (Figs. 2A1, A2, B1, B2; 3A1, A2, B1 and B2). In Ubá at 15, 22 and 29 dai, tissue proximal to the internal necrotic areas, as cortical parenchyma, xylem vessels, parenchyma cells and pith parenchyma in the stem sections exhibited strong autofluorescence using blue and UV light filter sets (Figs. 2D1, D2, F1, F2, H1, H2; 3D1, D2, F1, F2, H1 and H2). At the same evaluation times, the stem tissue of inoculated plants from Haden exhibited weak autofluorescence (Figs. 2C1, C2, E1, E2, G1, G2; 3C1, C2, E1, E2, G1 and G2).

X-ray microanalysis. The stem tissue from Haden and Ubá were colonized by *C. fimbriata* (Fig. 4A,B, C and D). At 22 dai, the peaks for insoluble S and Ca in Ubá stem tissue were approximately 15% and 30% higher when compared to the Haden (Fig. 4A1 and B1). At 29 dai, the peaks for S and Ca in the Ubá stem tissue were greater by approximately 17% and 72%, respectively when compared to the Haden (Fig. 4C1and D1). For all evaluation times, higher levels of deposition of S and Ca in the Ubá stem tissue were observed proximal to the inoculation point compared with the Haden (Fig. 4A2, A3, B2, B3, C2, C3, D2 and D3). At 22 dai, abundant amounts of fungal hyphae and chlamydospores (aleurioconidia) of *C. fimbriata* were visible in parenchyma cells of the stem tissue of both cultivars, but in Haden stem tissue, fungal hyphae had reached xylem vessels (Fig. 5A and B). The S and Ca peaks detected in the Ubá stem tissue, which was densely colonized by *C. fimbriata*, were higher by approximately 108% and 281%, respectively, compared to Haden (Fig. 5A1and B1). At 29 dai, xylem vessels were obstructed by the formation of tyloses in both Haden and Ubá (Fig. 5C and D). The S and Ca peaks from xylem vessels containing tyloses in the Ubá stem tissue were higher by 93% and 255%, respectively, than those in the Haden (Fig. 5C1and D1). Thus, at all evaluation times, levels of insoluble S and Ca deposition were higher in the cells colonized by *C.*

fimbriata and in xylem vessels containing tyloses in the Ubá stem tissue in comparison to Haden (Fig. 5A2, A3, B2, B3, C2, C3, D2 and D3).

Scanning electron microscopy. At 22 dai, chlamydospores had formed or were in the process of formation in cortical parenchyma of the stem tissue from both cultivars (Fig. 6A, A1, G and G1). In the Haden stem tissue, long fungal hyphae invaded xylem vessels, stimulating formation of a substantial amount of polysaccharide gel and tyloses (Fig. 6B, C, D and E). In the Ubá stem tissue, numerous chlamydospores were observed in parenchyma cells and xylem vessels (Fig. 6H, I, J, K and L). In xylem vessels of Ubá stem tissue, polysaccharide gels were infrequent (Fig. 6H, I, J, K and L). Fungal hyphae extensively colonized the pith parenchyma of Haden stem tissue (Fig. 6F), but were not observed in these same cells of Ubá (Fig. 6G, H, I, J, K and L). At 29 dai, several fungal hyphae, chlamydospores and perithecia-like structures were visible on the Haden stem tissue. These started from the stem region where inoculation occurred and progressed toward the cortical parenchyma and xylem vessels distal to the inoculation area (Fig. 7A, A1, B, C, C1, D and E). By comparison, on the Ubá the fungal structures were only observed in the cortical parenchyma and xylem vessels proximal to the inoculation area (Fig.7G, H, H1, I, I1, J, J1, K and L). Fungal hyphae extensively colonized the pith parenchyma of Haden (Fig. 7F), but were not observed in these same cells of Ubá (Fig. 7G, H, I, J, K and L).

Transmission electron microscopy. Fungal hyphae easily invaded fiber and parenchyma cells adjacent to xylem vessels in the stem tissue of the Haden (Fig. 8A, B, C, D and E). In the Ubá, fungal hyphae were often surrounded by dense amorphous granular material in fiber and parenchyma cells (Fig. 9A, B, C and D). Parenchyma cell walls in Haden showed signs of intense degradation after colonization by *C. fimbriata* (Fig. 8B, C, D and E). In opposite, the parenchyma cell walls of Ubá rarely were degraded and were encrusted by amorphous granular material (Fig. 9A, B, C and D). Long and thick fungal hyphae were often found in Haden stem tissue (Fig. 8), but were thin and faint and sometimes appeared dead in Ubá (Fig. 9). Fungal hyphae penetrated pit membranes and reached the xylem vessels in Haden (Fig. 8F and G), whereas in Ubá fungal colonization was impeded by the deposition of amorphous granular material (Fig. 9E and F). Fungal hyphae that reached xylem vessels in Ubá stem tissue were often surrounded by dense amorphous granular material and some appeared dead (Fig. 9E and G). In contrast,

fungal hyphae abundantly colonized the xylem vessels in Haden stem tissue (Fig. 8F and G).

DISCUSSION

This study provides direct evidence for differences in response to infection by *C. fimbriata* at the cellular level in two mango cultivars. Responses of Haden and Ubá to *C. fimbriata* infection were as a susceptible and resistant reaction, respectively, when inoculated and kept at greenhouse conditions. This reaction mirrored what has been observed in their performance under production field practices (41,46,56).

Tissue proximal to the internal necrotic areas in the stem sections obtained from Ubá had stronger autofluorescence compared to Haden. There are several published reports of autofluorescence around necrotic areas in the stem tissue of resistant plants attacked by vascular pathogens (2,7,9,21,43). In these reports, resistance is manifested by barrier zones that reduce the spread of the pathogens (2,7,9,21,43). Suberin, lignin and phenolic-like compounds are of great importance in barrier zones, as demonstrated in the interactions between American elm and *O. novo-ulmi* (2), white fir and *Phellinus pini* (9), trembling aspen and *Entoleuca mammata* (11), oilseed rape and *V. longisporum* (21), balsam poplar and *O. novo-ulmi* (43), jack pine and *Gremmeniella abietina* (49) and sugar maple and *Ceratocystis coerulescens* (53). Phenolic-like compounds, phytoalexins, suberin and lignin will autofluorescence when excited by near blue and UV light (2,7,9,21,29,43). Bishop and Cooper (7) observed strong autofluorescence of pea stem tissue from the accumulation of phenolics as a result of a hypersensitive reaction in response to the *F. oxysporum* f.sp. *pisi* attack. In the present study, the strong autofluorescence around the necrotic stem tissue obtained from Ubá in response to *C. fimbriata* infection is most likely due to of barrier zones infused with suberin, lignin and phenolic-like compounds. These compounds help prevent the spread of the fungus through the vascular system.

The peaks and deposition of bound or insoluble S and Ca in the stem tissue from Ubá attacked by *C. fimbriata* were always higher than those produced by tissue from Haden. It is known that higher levels of the chemical elements S and Ca in plant tissue can increase resistance to vascular pathogens (17). Cooper et al. (15) reported the presence of two phenolics, a triterpenoid and an elemental S, as cyclooctasulfur in the xylem vessels of the stem tissue of a resistant genotype of cacao in response to infection by *V. dahliae*. X-ray microanalysis also revealed a higher accumulation of S in the cells that were in close contact with hyphae of *V. dahlia* (15). Sugimoto et al. (52) found that soybean plants supplied with a high level of Ca showed reduced symptoms of Phytophthora stem rot. X-ray microanalysis also showed that Ca

crystals were found around the cambium and xylem in the stem tissue of soybean, suggesting the importance of Ca ion storage in maintaining long-term field resistance and reducing *P. sojae* penetration (52). In the present study, high levels of S in the stem tissue of Ubá were associated with putative antimicrobial activity against *C. fimbriata,* suggesting novel mechanism of defense for the interaction between mango plants and *C. fimbriata*. The high levels of Ca in the stem tissue from Ubá may also have contributed to the strength of the cell walls, which hampered *C. fimbriata* colonization.

Long fungal hyphae, chlamydospores and perithecia-like structures of *C. fimbriata* were found in abundance in stem tissue of the susceptible Haden based on scanning electron microscopic observations. The same *C. fimbriata* structures were less apparent in resistant Ubá. The colonization of stem tissue of susceptible cultivars by vascular pathogens is enhanced and their xylem vessels are often obstructed by fungal hyphae and polysaccharide gels and the formation of tyloses (7,8,14,37,44). The resistance of trees to vascular pathogens results from their ability to restrict pathogens to a few cells (20) based on pre- and/or post-formed defense mechanisms (6,9,20,32,43). In the present study, the intense autofluorescence, stronger peaks and depositions of elemental S and Ca near inoculation areas in the stem tissue of Ubá appears to act as a barrier preventing radial spread of hyphae from reaching the pit parenchyma.

Transmission electron microscopy revealed long, thickened fungal hyphae in fiber and parenchyma cells as well as in the xylem vessels of Haden. However, in Ubá hyphae were thin and faint in these same cells and were often surrounded or trapped in dense amorphous granular material, and often hyphae appeared to be dead. The presence of amorphous material, frequently reported to consist of phenolic-like compounds, is a typical feature of cellular defense used by many plant species to cope with fungal infection (4,5,7,8,21,26,35,45). Others have reported the occurrence of dead hyphae surrounded or trapped in amorphous material (4,5,7,8,35,38,45). This phenomena is found in numerous plant species (4,5,7,8,35,38,45). The fungitoxic effect of most phenolics is attributed to their interaction with lipids or phospholipids, which increases fungal membrane permeability, leakage of hyphal contents and cytoplasm aggregation (50). In mango fruits, many antimicrobial phenolic compounds, like catechin, coumaric acid, gallic acid, hydroxybenzoic acid, isomangiferin, kaempferol, mangiferin, protocatechuic acid, quercetin, sinapic acid

and shikimic acid, have been reported (31,42). Therefore, the reduced fungal colonization of the stem tissue in Ubá was most likely due to the intense accumulation of phenolic-like compounds surrounding the fungal hyphae and resulting in stronger autofluorescence and greater S deposition in close proximity to these hyphae.

The parenchyma cell walls of the Haden colonized by fungal hyphae often showed strong signs of degradation. In contrast, the parenchyma cell walls of Ubá were less degraded and were frequently encrusted by amorphous granular material. Degradation of cell walls is a typical feature reported in interactions between peas and *F. oxysporum* f.sp. *pisi* (7), tomatoes and *V. albo-atrum* (8) and *F. oxysporum* f.sp. *lycopersici* (33) and American elm and *O. ulmi* (35). Wall degradation is often attributed to release into the vascular fluid of cell wall-degrading enzymes produced by pathogens (3,13,33,44). Uritani and Stahmann (54) reported that *C. fimbriata* produces pectinases in culture medium and in cells of the sweet potato that the fungus has penetrated. In the present study, the absence of damage to cell walls of the Ubá was most likely due to the protective nature of the amorphous granular material that prevented degradation by fungal hyphae and protected the host cell walls.

High levels of insoluble Ca were found in Ubá stem tissue colonized by *C. fimbriata*. High levels of Ca are associated with resistance to cell wall-degrading enzymes produced by pathogens (3,13,28,39). This is thought to occur because Ca bridges form between carboxyls of adjacent pectic chains in the host cell walls making these well less accessible to the lytic enzymes released by the pathogens (3,13,28,39). Corden and Edgington (16) found that the resistance of tomato plants to *F. oxysporum* f.sp. *lycopersici* was due to an increase in calcium pectate that reduced the susceptibility of the pectin to degradation by the pectic enzymes produced by the vascular pathogen. Most likely the tissue of Ubá containing high levels of Ca were more resistant to mango wilt because the cell wall strength hampered activity of cell wall-degrading enzymes of *C. fimbriata*.

Fungal hyphae penetrated the pit membranes of the stem tissue of Haden whereas in tissue of Ubá, fungal penetration was often impeded by amorphous granular material. The pit membrane has a middle lamella and a primary cell wall designed to facilitate water flow between neighboring conduits and to prevent spread of gas bubbles causing a gas embolism (25). Various vascular pathogens can degrade the pit

membrane and spread through intervessel colonization (8,35,36). Pit penetration in susceptible tomato cultivars was achieved by constricted hyphae of *F. oxysporum* f.sp. *lycopersici* and *V. albo-atrum* without impediment by their hosts (8). However, in resistant plants protective layers adjacent to pit membranes in parenchyma cells adjacent to the xylem vessels were formed in response to attack by several vascular pathogens (8,35,36,38). Often, these layers of amorphous material are not found in non-infected vascular tissue, but in infected tissue layers of amorphous materials protect vessels of adjacent tissue from pathogen invasion (8,35,36,38). Generally, the difference between resistant and susceptible plants is related to the degree of phenolic infusion, lignification or incorporation of Ca ions into pit membrane (8,35). In the present study, the deposition of phenolic-like compounds in the pit membranes and high levels of S and Ca in the stem tissue of Ubá helped explain the reduced *C. fimbriata* colonization in the xylem vessels and the absence of wilted plants.

In conclusion, marked differences at the cellular level in the stem tissue of the two mango cultivars during the infection process of *C. fimbriata* were noticed. In the resistant Ubá, there was less fungal colonization, reduced stem tissue necrosis and absence of wilted plants when compared to the susceptible cv. Haden. These results revealed that the barrier zones, deposition of S and Ca and accumulation of phenolic-like compounds played a pivotal role in the defense of mango plants against infection by *C. fimbriata.* These results indicate that mango wilt resistance through a plant breeding program and nutritional enhancement are feasily possible.

ACKNOWLEDGMENTS

Prof. Fabrício A. Rodrigues thanks CNPq for his fellowship. Mr. Leonardo Araujo was supported by CNPq. The authors thank the “Núcleo de Microscopia e Microanálise” of the Federal University of Viçosa for the use of the equipment. The authors thank Prof. Acelino C. Alfenas and Mr. Leonardo S. S. Oliveira for kindly providing the isolate of *C. fimbriata* used in this study. The authors gratefully acknowledge Professors Lawrence E. Datnoff and Richard J. Zeyen for their review and many suggestions that have significantly improved the manuscript. This study was supported by a grant from Vale S.A. to Prof. F. A. Rodrigues.

LITERATURE CITED

1. Al-Sadi, A. M., Al-Ouweisi, F. A., Al-Shariani, N. K., Al-Adawi, A. O., Kaplan, E. J., and Deadman, M. L. (2010) Histological changes in mango seedlings following infection with *Ceratocystis manginecans*, the cause of mango decline. J. Phytopathol. 158:738-743.
2. Aoun, M., Rioux, D., Simard, M., and Bernier, L. 2009. Fungal colonization and host defense reactions in *Ulmus americana* callus cultures inoculated with *Ophiostoma novo-ulmi*. Phytopathology 99:642-650.
3. Bateman, D. F., and Millar, R. L. 1966. Pectic enzymes in tissue degradation. Annu. Rev. Phytopathol. 4:119-144.
4. Bélanger, R. R., Benhamou, N., and Menzies, J. G. 2003. Cytological evidence of an active role of silicon in wheat resistance to powdery mildew (*Blumeria graminis* f.sp. *tritici*). Phytopathology 93:402-412.
5. Benhamou, N., and Bélanger, R. R. 1998. Benzothiadiazole-mediated induced resistance to *Fusarium oxysporum* f.sp. *radicis-lycopersici* in tomato. Plant Physiol. 118:1203-1212.
6. Biggs, A. R. 1992. Anatomical and physiological responses of bark tissues to mechanical injury. Pages 13-36 in: Defense Mechanisms of Woody Plants Against Fungi. R. A. Blanchette, and A. T. Biggs, eds. Springer-Verlag, Berlin.
7. Bishop, G. D., and Cooper, R. M. 1983a. An ultrastructural study of root invasion in three vascular wilt diseases. Physiol. Plant Pathol. 22:15-27.
8. Bishop, G. D., and Cooper, R. M. 1983b. An ultrastructural study of vascular colonization in three vascular wilt diseases I. Colonization of susceptible cultivars. Physiol. Plant Pathol. 23:323-343.
9. Blanchette, R. A. 1992. Anatomical responses of xylem to injury and invasion by fungi. Pages 76-95 in: Defense Mechanisms of Woody Plants Against Fungi. R. A. Blanchette, and A. T. Biggs, eds. Springer-Verlag, Berlin.
10. Bozzola, J. J., and Russell, L. D. 1999. Electron microscopy: principles and techniques for biologists. 2nd Ed. Jones and Bartlett Publishers, Boston. 670 pp.
11. Bucciarelli, B., Ostry, M. E., Fulcher, R. G., Anderson, N. A., and Vance, C. P. 1999. Histochemical and microspectrophotometric analyses of early wound responses of resistant and susceptible *Populus tremuloides* inoculated with *Entoleuca mammata* (= *Hypoxylon mammatum*). Can. J. Bot. 77:548-555.

12. Carvalho, C. R. L., Rossetto, C. J., Mantovani, D. M. B., Morgano, M. A., Castro J. V., and Bortoletto N. 2004. Avaliação de cultivares de mangueira selecionadas pelo Instituto Agronômico de Campinas comparadas a outras de importância comercial. Rev. Bras. Frutic. 26:264-271.

13. Collmer, A., and Keen N. T. 1986. The role of pectic enzymes in plant pathogenesis. Annu. Rev. Phytopathol. 24:383-409.

14. Cooper, R. M., and Wood R. K. S. 1974. Scanning electron microscopy of *Verticillium albo-atrum* in xylem vessels of tomato plants. Physiol. Plant Path. 4:443-446.

15. Cooper, R. M., Resende, M. L. V., Flood, J., Rowan, M. G., Beale, M. H., and Potter, U. 1996. Detection and cellular localization of elemental sulphur in disease resistant genotypes of *Theobroma cacao*. Nature 379:159-162.

16. Corden, M. E., and Edgington, L. V. 1960. A calcium requirement for growth-regulator-induced resistance to Fusarium wilt of tomato. Phytopathology 50:625-626.

17. Datnoff, L. E., Elmer, W. H., and Huber, D. M. 2007. Mineral Nutrition and Plant Disease. APS Press: The American Phytopathological Society. Saint Paul, Minnesota, U.S.A. 278 pp.

18. Dhingra, O. D., and Sinclair, J. B. 1995. Basic Plant Pathology Methods. Boca Raton, Lewis Publisher. 448 pp.

19. Dixon, R. A., and Paiva, N. L. 1995. Stress induced phenylpropanoid metabolism. Plant Cell 7:1085-1097.

20. Duchesne, L. C., Hubbes, M., and Jeng, R. S. 1992. Biochemistry and molecular biology of defense reactions in the xylem of angiosperm trees. Pages 133-142 in: Defense Mechanisms of Woody Plants Against Fungi. R. A. Blanchette, and A. T. Biggs, eds. Springer-Verlag, Berlin.

21. Eynck, C., Koopmann, B., Karlovsky, P., and von Tiedemann, A. 2009. Internal resistance in winter oilseed rape inhibits systemic spread of the vascular pathogen *Verticillium longisporum*. Phytopathology 99:802-811.

22. FAO, 2013. Medium-term prospects for agricultural Commdities. In: Food and Agriculture Organization of the United Nations. http://www.fao.org/docrep/006/y5143e/y5143e1a.htm.

23. Ferreira, E. M., Harrington, T. C., Thorpe, D. J., and Alfenas, A. C. 2010. Genetic diversity and interfertility among highly differentiated populations of *Ceratocystis fimbriata* in Brazil. Plant Pathol. 59:721-735.

24. Goldstein, J., Newbury, D., Joy, D., Lyman, C., Echlin, P., Lifshin, E., Sawyer, L., and Michael, J. 2003. Scanning electron microscopy and X-ray microanalysis. 3rd ed. Kluwer Academic/Plenum Publishers, New York. 690 pp.

25. Gortan, E., Nardini, A., Salleo, S., and Jansen, S. 2011. Pit membrane chemistry influences the magnitude of ion-mediated enhancement of xylem hydraulic conductance in four Lauraceae species. Tree Physiol. 31:48-58.

26. Hall, C., Heath, R., and Guest, D. I. 2011. Rapid and intense accumulation of terpenoid phytoalexins in infected xylem tissues of cotton (*Gossypium hirsutum*) resistant to *Fusarium oxysporum* f.sp. *vasinfectum.* Physiol. Mol. Plant Pathol. 76:182-188.

27. Haneklaus, S., Bloem, E., and Schnug, E. 2007. Sulfur and plant disease. Pages 101-118 in: Mineral Nutrition and Plant Disease. L. E. Datnoff, W. H. Elmer, and D. M. Huber, eds. Saint Paul Minnesota, U.S.A. APS Press.

28. Huang, J. S. 2001. Plant Pathogenesis and Resistance: Biochemistry and Physiology of Plant-Microbe Interactions. Kluwer Academic Publishers. Norwell, Madison. 691 pp.

29. Koga, H., Zeyen, R. J., Bushnell, W. R., and Ahlstrand, G. G. 1988. Hypersensitive cell death, autofluorescence, and insoluble silicon accumulation in barley leaf epidermal cells under attack by *Erysiphe graminis* f.sp. *hordei.* Physiol. Mol. Plant Path. 32:395-409.

30. Lecourieux, D., Ranjeva, R., and Pugin, A. 2006. Calcium in plant defence-signalling pathways. New Phytol. 171:249-269.

31. Liu, F. X., Fu, S. F., Bi, X. F., Chen, F., Liao, X. J., Hu, X. S. and Wu, J. H. 2013. Physico-chemical and antioxidant properties of four mango (*Mangifera indica* L.) cultivars in China. Food Chem. 138:396-405.

32. Merrill, W. 1992. Mechanisms of resistance to fungi in woody plants: A historical perspective. Pages 1-11 in: Defense Mechanisms of Woody Plants Against Fungi. R. A. Blanchette, and A. T. Biggs, eds. Springer-Verlag, Berlin.

33. Mussell, H. W., and Green, R. J. J. 1970. Host colonization and polygalacturonase production by two tracheomycotic fungi. Phytopathology 60:192-195.

34. Nicholson, R. L., and Hammerschmidt, R. 1992. Phenolic compounds and their role in disease resistance. Annu. Rev. Phytopathol. 30:369-389.

35. Ouellette, G. B., and Rioux, D. 1992. Anatomical and physiological aspects of resistance to Dutch Elm disease. Pages 257-301 in: Defense Mechanisms of Woody Plants Against Fungi. R. A. Blanchette, and A. T. Biggs, eds. Springer-Verlag, Berlin.

36. Ouellette, G. B., Rioux, D., Simard, M., and Cherif, M. 2004. Ultrastructural and cytochemical studies of host and pathogens in some fungal wilt diseases: retro- and introspection towards a better understanding of DED. Invest. Agrar. Sist. Recur. For. 13:119-145.

37. Parke, J. L., Oh, E., Voelker, S., Hansen, E. M., Buckles, G., and Lachenbruch, B. 2007. *Phytophthora ramorum* colonizes tanoak xylem and is associated with reduced stem water transport. Phytopathology 97:1558-1567.

38. Pegg, G. F. 1976. Transmission electron microscopy of *Verticillium albo-atrum* hyphae in xylem vessels of tomato plants. Physiol. Plant Pathol. 8:22l-224.

39. Rahman, M., and Punja, Z. K. 2007. Calcium and plant disease. Pages 79-93 in: Mineral Nutrition and Plant Disease. L. E. Datnoff, W. H. Elmer, and D. M. Huber, eds. Saint Paul Minnesota, U.S.A. APS Press.

40. Ribeiro, I. J. A., Rossetto, C. J., Sabino, J. C., and Gallo, P. B. 1986. Seca da mangueira: VIII. Resistência de porta-enxertos de mangueira ao fungo *Ceratocystis fimbriata* Ell. & Halst. Bragantia 45:317-322.

41. Ribeiro, I. J. A. 2005. Doenças da mangueira (*Mangifera indica L.*). Pages 457-465 in: Manual de Fitopatologia: Doenças das Plantas Cultivadas. H. Kimati, L. Amorim, A. Bergamin-Filho, L. E. A. Camargo, and J. A. M. Rezende, eds. Agronômica Ceres, São Paulo.

42. Ribeiro, S. M. R., Barbosa, L. C. A., Queiroz, J. H., Knodler, M., and Schieber, A. 2008. Phenolic compounds and antioxidant capacity of Brazilian mango (*Mangifera indica* L.) varieties. Food Chem.110:620-626.

43. Rioux, D., and Baayen, R. P. 1997. A suberized perimedullary reaction zone in *Populus balsamifera* novel for compartmentalization in trees. Trees 11:389-403.

44. Rioux, D., Nicole, M., Simard, M., and Ouellette, G. B. 1998. Immunocytochemical evidence that secretion of pectin occurs during gel (gum) and tylosis formation in trees. Phytopathology 88:494-505.

45. Rodrigues, F. A., Benhamou, N., Datnoff, L. E., Jones, J. B., and Bélanger, R. R. 2003. Ultrastructural and cytochemical aspects of silicon-mediated rice blast resistance. Phytopathology 93:535-546.

46. Rossetto, C. J., Ribeiro, I. J. A., Igue, T., and Gallo, P. B. 1996. Seca-da-mangueira XV. Resistência varietal a dois isolados de *Ceratocystis fimbriata*. Bragantia 55:117-121.

47. Scalet, M., Crivellato, E., and Mallardi, F. 1989. Demonstration of phenolic compounds in plant tissues by an osmium-iodide postfixation procedure. Stain Technol. 64:273-290.

48. Shaner, G., and Finney R. E. 1977. The effect of nitrogen fertilization on the expression of slow-mildewing resistance in knox wheat. Phytopathology 70:1183-1186.

49. Simard, M., Rioux, D., and Laflamme, G. 2001. Formation of ligno-suberized tissues in jack pine resistant to the European race of *Gremmeniella abietina*. Phytopathology 91:1128-1140.

50. Southerton, S. G., and Deverall, B. J. 1990. Histochemical and chemical evidence for lignin accumulation during the expression of resistance to leaf rust fungi in wheat. Physiol. Mol. Plant Pathol. 36:483-494.

51. Souza, A. G. C., Rodrigues, F. A., Maffia, L. A., and Mizubuti, E. S. G. 2011. Infection process of *Cercospora coffeicola* on coffee leaf. J. Phytopathol. 159:6-11.

52. Sugimoto, T., Watanabe, K., Yoshida, S., Aino, M., Furiki, M., Shiono, M., Matoh, T., and Biggs, A. R. 2010. Field application of calcium to reduce Phytophthora stem rot of soybean, and calcium distribution in plants. Plant Dis. 94:812-819.

53. Tippett, J. T., and Shigo, A. L. 1981. Barrier zone formation: a mechanism of tree defense against vascular pathogens. Iawa Bull. 4:163-168.

54. Uritani, I., and Stahmann, M. A. 1961. Pectolytic enzymes of *Ceratocystis fimbriata*. Phytopathology 51:277-285.

55. Van Wyk, M., Al Adawi, A. O., Khan, I. A., Deadman, M. L., Al Jahwari, A. A., Wingfield, B. D., Ploetz, R., and Wingfield, M. J. 2007. *Ceratocystis manginecans* sp. nov., causal agent of a destructive mango wilt disease in Oman and Pakistan. Fungal Divers. 27:213-230.

56. Viégas, A. P. 1960. Seca da mangueira. Bragantia 19:163-182.

57. Williams, J. S., Hall, S. A., Hawkesford, M. J., Beale, M. H., and Cooper, R. M. 2002. Elemental sulfur and thiol accumulation in tomato and defense against a fungal vascular pathogen. Plant Physiol. 128:150-159.

58. Zeyen, R. J., Ahlstran, G. G., and Carver, T. L. W. 1993. X-ray microanalysis of frozen-hydrated, freeze-dried, and critical point dried leaf specimens: determination of soluble and insoluble chemical elements at *Erysiphe graminis* epidermal cell papilla sites in barley isolines containing *M1-o* and *ml-o* alleles. Can. J. Bot. 71:284-296.

LIST OF TABLE AND FIGURES

TABLE 1. Area under upward relative lesion length progress curve (AUURLLPC), area under downward relative lesion length progress curve (AUDRLLPC), area under radial fungal colonization progress curve (AURFCPC) and area under wilted leaf progress curve (AUWLPC) for plants from the mango cultivars Haden (susceptible) and Ubá (resistant) inoculated with *Ceratocystis fimbriata*.

Cultivars	Variables			
	AUURLLPC	AUDRLLPC	AURFCPC	AUWLPC
Haden	592.4	183.4	974.4	340.2
Ubá	104.7	107.4	394.6	0.0
F values	0.008**	0.029*	0.000**	0.000**

* and ** = significant at 5 and 1% of probability, respectively.

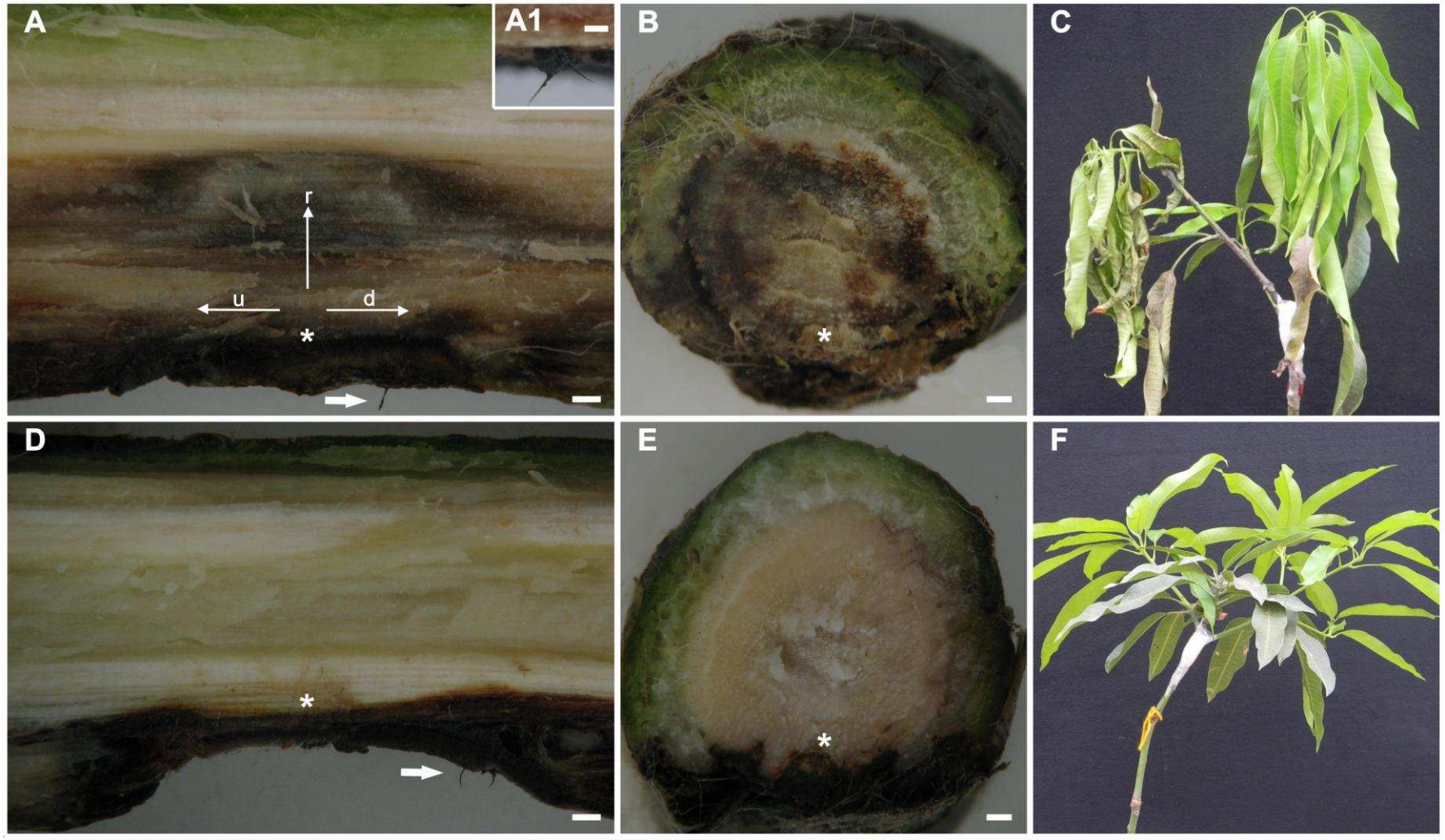

Fig. 1

Fig. 1. Internal necrotic tissue caused by *Ceratocystis fimbriata* infection in longitudinal (A and D) and transverse (B and E) stem sections and wilting symptoms (A and F) in mango plants from the susceptible cv. Haden (A, B and C) and resistant cv. Ubá (D, E and F) at 22 days after inoculation. Asterisks (*) indicate the stem region where the fungal inoculation occurred and from which the upward (u), downward (d) and radial (r) *C. fimbriata* colonization were observed as detailed in A. The formation of perithecia of *C. fimbriata* was observed at the inoculation point (arrow in A and C). In A1, perithecia of *C. fimbriata* are shown at a higher magnification. Scale bars: 1000 µm (A, B, D and E) and 500 µm (A1).

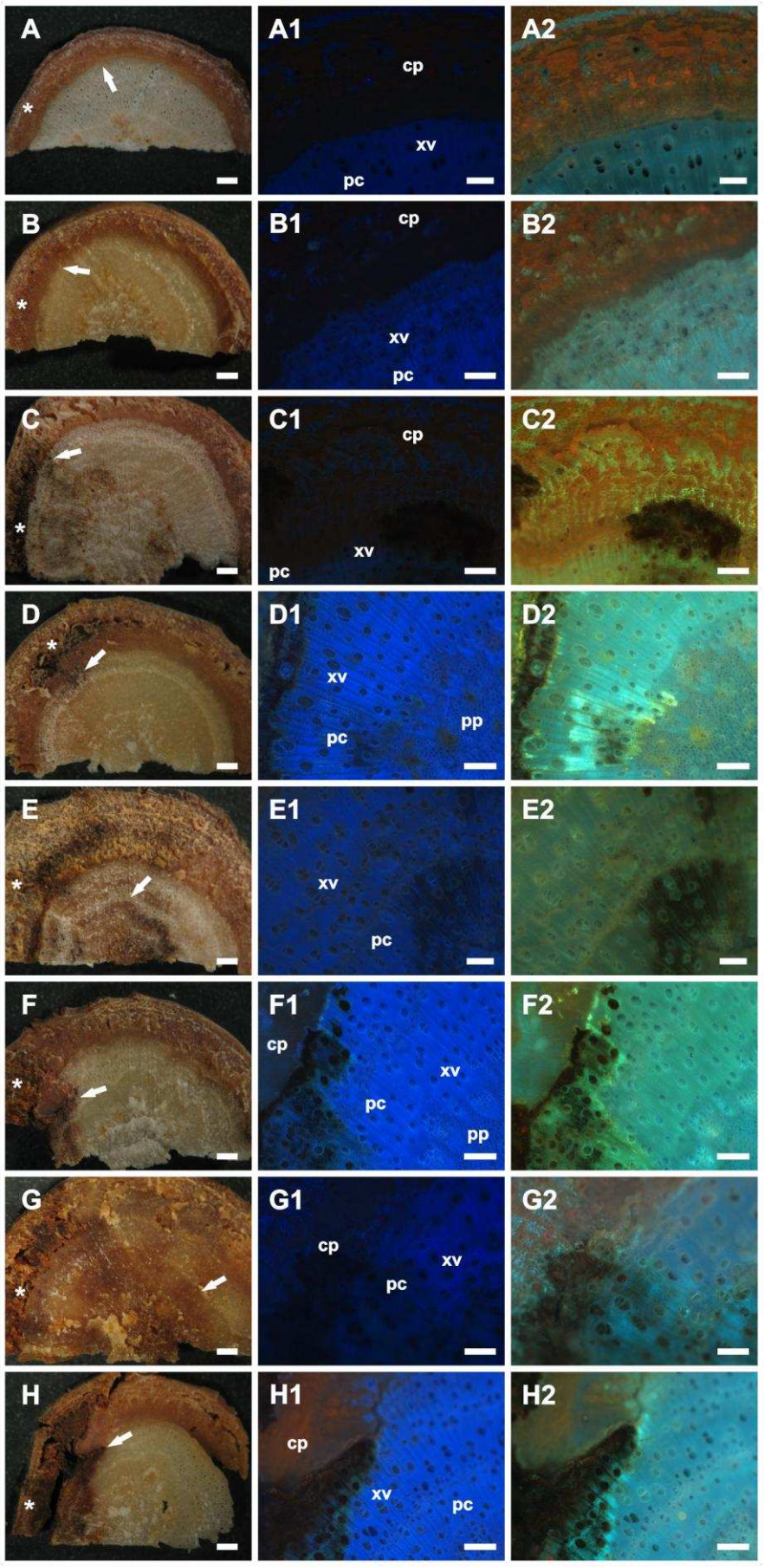
A
A1
cp
xv
pc
A2
B
B1
cp
xv
pc
B2
C
C1
cp
xv
pc
C2
D
D1
xv
pp
pc
D2
E
E1
xv
pc
E2
F
F1
cp
xv
pc
pp
F2
G
G1
cp
xv
pc
G2
H
H1
cp
xv
pc
H2

Fig. 2

Fig. 2. Stem sections of non-inoculated plants of cultivars Haden (A, A1, A2) and Ubá (B, B1 and B2). Symptoms of internal necrotic tissue (C, D, E, F, G and H) and fluorescence microscopy images in transverse stem sections from mango plants of cultivars Haden (C1, C2, E1, E2, G1 and G2) and Ubá (D1, D2, F1, F2, H1 and H2) at 15 (C, C1, C2, D, D1 and D2), 22 (E, E1, E2, F, F1 and F2) and 29 (G, G1, G2, H, H1 and H2) days after inoculation (dai) with *Ceratocystis fimbriata*. Asterisks (*) in A, B, C, D, E, F, G and H indicate the stem region where the wound for fungal inoculation was made. Arrows indicate the stem region where autofluorescence in non-inoculated (A, A1, A2, B, B1 and B2) and inoculated plants was recorded (C, C1, C2, D, D1, D2, E, E1, E2, F, F1, F2, G, G1, G2, H, H1 and H2) when observed with blue (395-400 nm excitation) and UV light (365 nm excitation) filter sets. Cortical parenchyma (cp), parenchyma cells (pc), pith parenchyma (pp) and xylem vessels (xv). Scale bars in A, B, C, D, E, F, G and H = 1000 µm and in A1, A2, B1, B2, C1, C2, D1, D2, E1, E2, F1, F2, G1, G2, H1 and H2 = 250 µm.

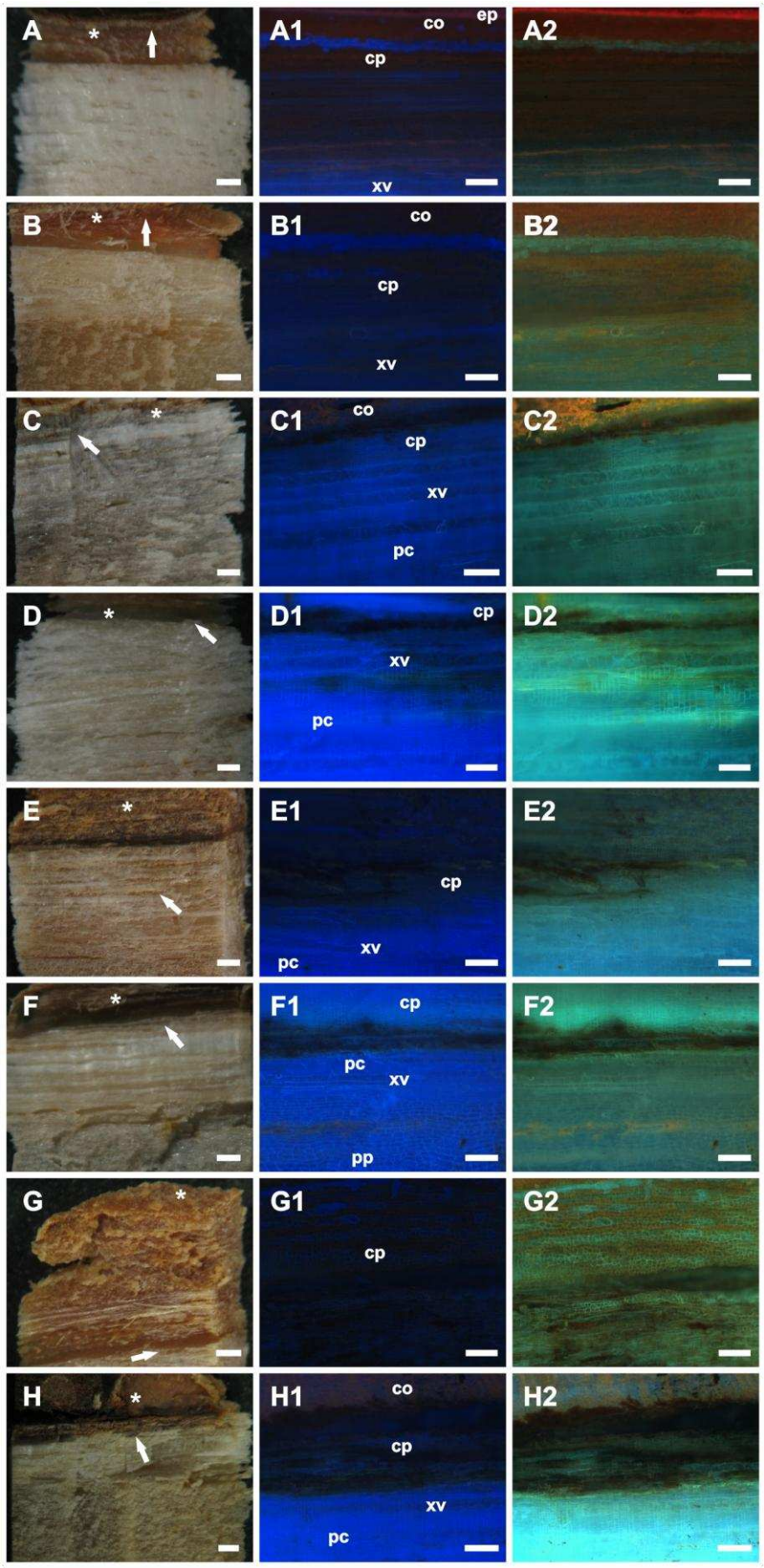
A
A1
co
ep
cp
xv
A2
B
B1
co
cp
xv
B2
C
C1
co
cp
xv
pc
C2
D
D1
cp
xv
pc
D2
E
E1
cp
xv
pc
E2
F
F1
cp
pc
xv
pp
F2
G
G1
cp
G2
H
H1
co
cp
xv
pc
H2

Fig. 3

Fig. 3. Stem sections of non-inoculated plants of cultivars Haden (A, A1, A2) and Ubá (B, B1 and B2). Symptoms of internal necrotic tissue (C, D, E, F, G and H) and fluorescence microscopy images in longitudinal stem sections from mango plants of cultivars Haden (C1, C2, E1, E2, G1 and G2) and Ubá (D1, D2, F1, F2, H1 and H2) at 15 (C, C1, C2, D, D1 and D2), 22 (E, E1, E2, F, F1 and F2) and 29 (G, G1, G2, H, H1 and H2) days after inoculation (dai) with *Ceratocystis fimbriata*. Asterisks (*) in A, B, C, D, E, F, G and H indicate the stem region where the wound for fungal inoculation was made. Arrows indicate the stem region where autofluorescence in non-inoculated (A, A1, A2, B, B1 and B2) and inoculated plants was recorded (C, C1, C2, D, D1, D2, E, E1, E2, F, F1, F2, G, G1, G2, H, H1 and H2) when observed with blue (395-400 nm excitation) and UV light (365 nm excitation) filter sets. Collenchyma (co), cortical parenchyma (cp), epidermis (ep), parenchyma cells (pc), pith parenchyma (pp) and xylem vessels (xv). Scale bars in A, B, C, D, E, F, G and H = 1000 µm and in A1, A2, B1, B2, C1, C2, D1, D2, E1, E2, F1, F2, G1, G2, H1 and H2 = 250 µm.

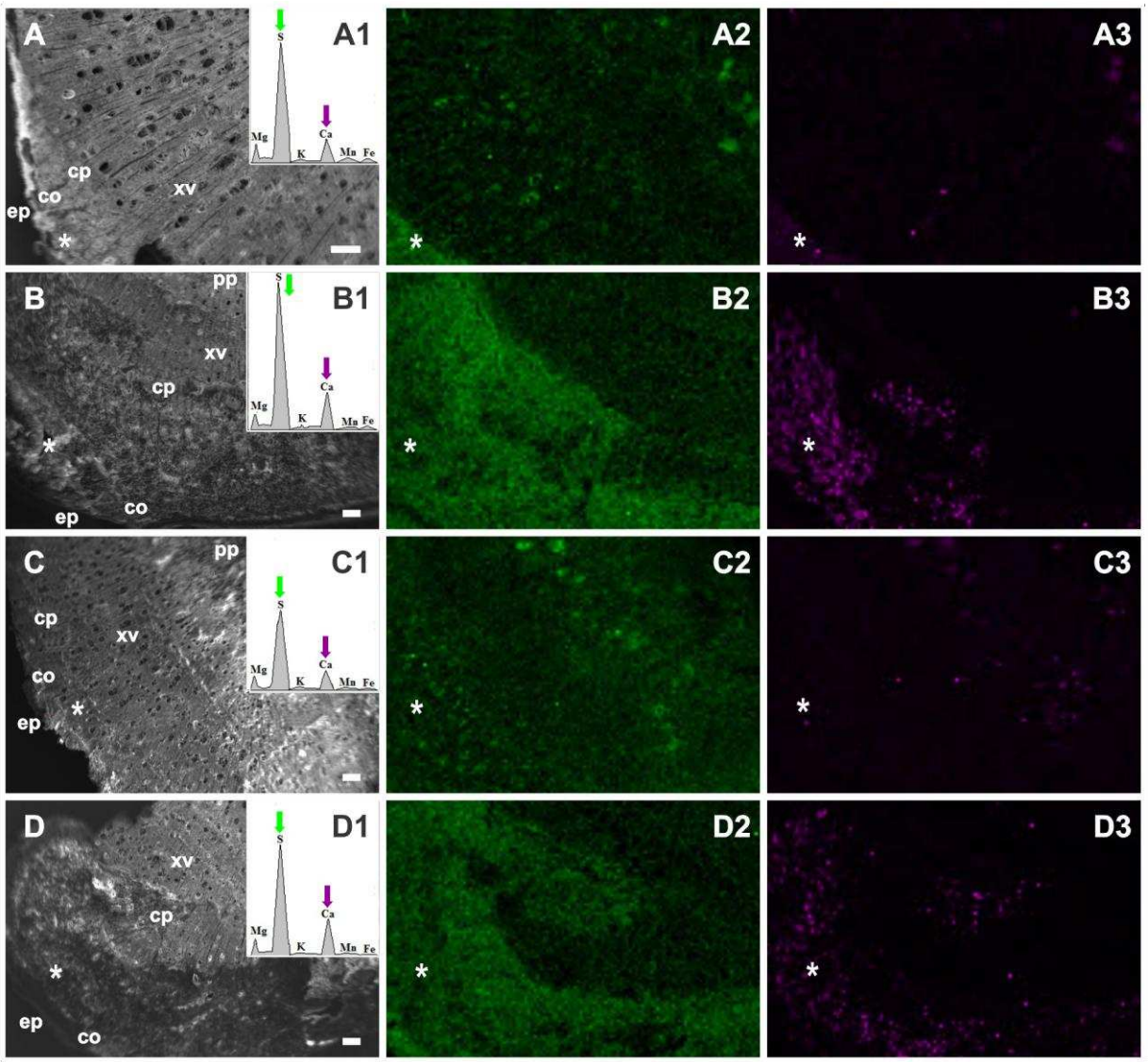

Fig. 4

Fig. 4. Scanning electron micrographs (A, B, C and D), X-ray emission spectra (A1, B1, C1 and D1) and corresponding X-ray maps for sulfur (S) (A2, B2, C2 and D2) and calcium (Ca) (A3, B3, C3 and D3) in transverse stem tissue sections of mango plants from cv. Haden (A and C) and Ubá (B and D) at 22 (A and B) and 29 (C and D) days after inoculation (dai) with *Ceratocystis fimbriata* (asterisks). A, B, C and D: Colonization of the epidermis, collenchyma, cortical parenchyma, xylem vessels and pith parenchyma by *C. fimbriata* in the stem tissue. Higher peaks for S (green arrow) and Ca (purple arrow) were detected in the stem tissue of plants from Haden (A1= 22 dai, S: 242.4, Error (E): 1.1; Ca: 52.7, E: 1.4; C1 = 29 dai, S: 176.8, E: 1.7; Ca: 39.8, E: 1.3) and Ubá (B1 = 22 dai, S: 279.0, E: 1.9; Ca: 68.3, E: 1.4; D1 = 29 dai, S: 206.9, E: 1.7; Ca: 70.5, E: 1.1) compared with other chemical elements. In the X-ray maps, green and purple fluorescent dots correspond to the accumulation of S and Ca, respectively, in the stem tissue of plants from Haden (A2, A3, C2 and C3) and Ubá (B2, B3, D2 and D3). Black is the absence of S and Ca. Collenchyma (co), cortical parenchyma (cp), epidermis (ep), iron (Fe), magnesium (Mg), manganese (Mn), parenchyma cells (pc), pith parenchyma (pp), potassium (K) and xylem vessels (xv). Scale bars = 200 µm.

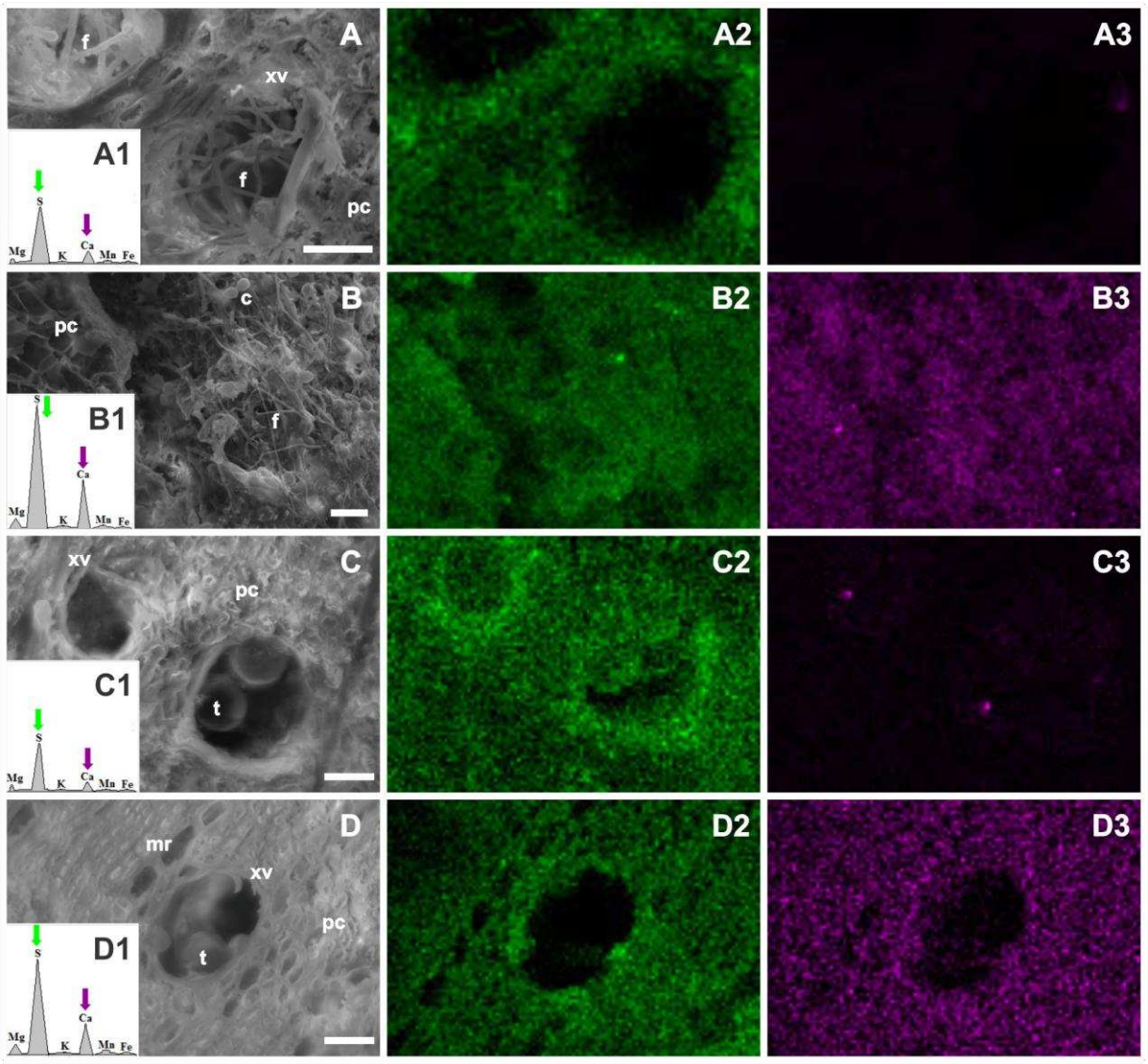
A
f
xv
A1
f
pc
S
Mg
K
Ca
Mn
Fe
A2
A3
B
c
pc
B1
f
B2
B3
C
xv
pc
C1
t
C2
C3
D
mr
xv
pc
D1
t
D2
D3

Fig. 5

Fig. 5. Scanning electron micrographs (A, B, C and D), X-ray emission spectra (A1, B1, C1 and D1) and corresponding X-ray maps for sulfur (S) (A2, B2, C2 and D2) and calcium (Ca) (A3, B3, C3 and D3) in transverse stem tissue sections of mango plants from cv. Haden (A and C) and Ubá (B and D) at 22 (A and B) and 29 (C and D) days after inoculation (dai) with *Ceratocystis fimbriata*. A: Hyphae of *C. fimbriata* extensively colonized the xylem vessels. B: Fungal hyphae grew abundantly in the parenchyma cells. C and D: The xylem vessels in the stem tissue of plants from Haden and Ubá were obstructed by the formation of tyloses at 29 dai. Higher peaks of S (green arrow) and Ca (purple arrow) were detected in the stem tissue of Haden (A1 = 22 dai, S: 120.3, Error (E): 1.2; Ca: 25.2, E: 0.8; C1 = 29 dai, S: 89.2, E: 1.1; Ca: 16.8, E: 0.8) and Ubá (B1 = 22 dai, S: 250.8, E: 1.8; Ca: 96.1, E: 1.3; D1 = 29 dai, S: 171.7, E: 1.6; Ca: 59.7, E: 1.1) compared with other chemical elements. In the X-ray maps, green and purple fluorescent dots correspond to the accumulation of S and Ca, respectively, in the stem tissue of plants from Haden (A2, A3, C2 and C3) and Ubá (B2, B3, D2 and D3). Black is the absence of S and Ca. Chlamydospores (c), fungal hyphae (f), iron (Fe), magnesium (Mg), manganese (Mn), medullary radius (mr), parenchyma cells (pc), potassium (K), tyloses (t) and xylem vessels (xv). Scale bars = 30 µm.

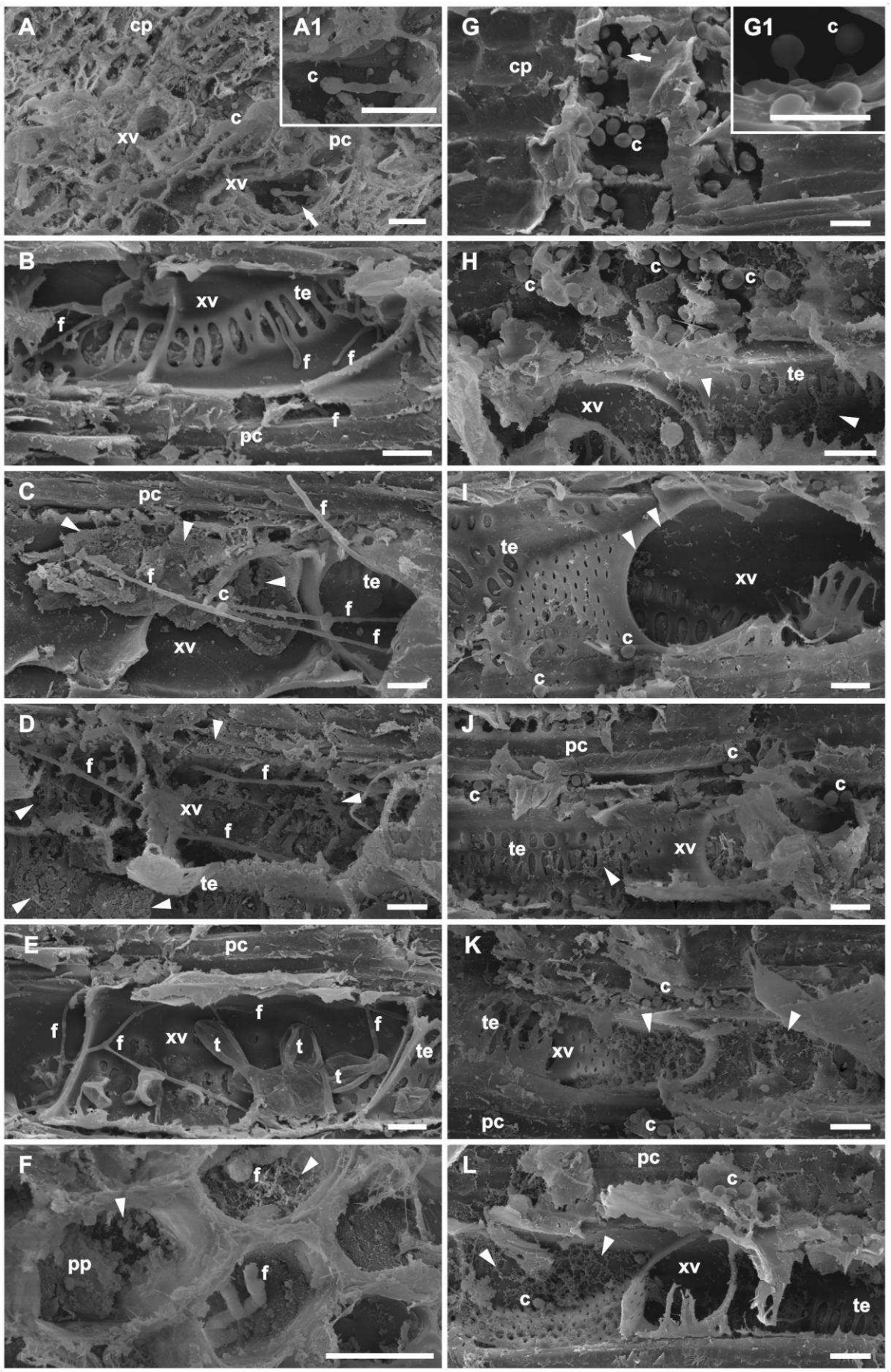
A
cp
A1
c
xv
c
pc
xv
G
cp
G1
c
c
B
xv
te
f
f
f
f
pc
H
c
c
c
te
xv
C
pc
f
f
c
te
f
f
xv
I
te
xv
c
c
D
f
f
xv
f
te
J
pc
c
c
c
te
xv
E
pc
f
f
f
f
xv
t
t
t
te
K
c
te
xv
pc
c
F
f
pp
f
L
pc
c
xv
c
te

Fig. 6

Fig. 6. Scanning electron micrographs of transverse (A and F) and longitudinal (B, C, D, E, G, H, I, J, K and L) sections of stem tissue from the mango cultivars Haden (A, B, C, D, E and F) and Ubá (G, H, I, J, K and L) at 22 days after inoculation with *Ceratocystis fimbriata*. A and A1: Chlamydospores (aleurioconidia) already formed or in the process of formation (arrow) were observed in the cortical parenchyma and in the xylem vessels. B: Fungal hyphae colonized the parenchyma cells and the xylem vessels. In the xylem vessels, fungal hyphae in tracheal elements and in adjacent areas can be observed. C and D: Long fungal hyphae and chlamydospores grew abundantly in the xylem vessels that were also obstructed by intense deposition of polysaccharide gels (arrowheads). E: Xylem vessels were obstructed by long fungal hyphae and large tyloses. F: Hyphae of *C. fimbriata* extensively colonized the pit parenchyma. Polysaccaride gels (arrowheads) were observed in certain cells of the pit parenchyma. G and G1: Many chlamydospores already formed or in process of formation (arrow) were observed in the cortical parenchyma. H, I, J, K and L: Chlamydospores were observed in the parenchyma cells and in the xylem vessels, and several appeared to have formed in chains. Polysaccharide gels (arrowheads) were rarely deposited in the xylem vessels. Chlamydospores (c), cortical parenchyma (cp), fungal hyphae (f), parenchyma cells (pc), pith parenchyma (pp), polysaccharide gels (pg), tracheal elements (te), tyloses (t) and xylem vessels (xv). Scale bars = 20 µm.

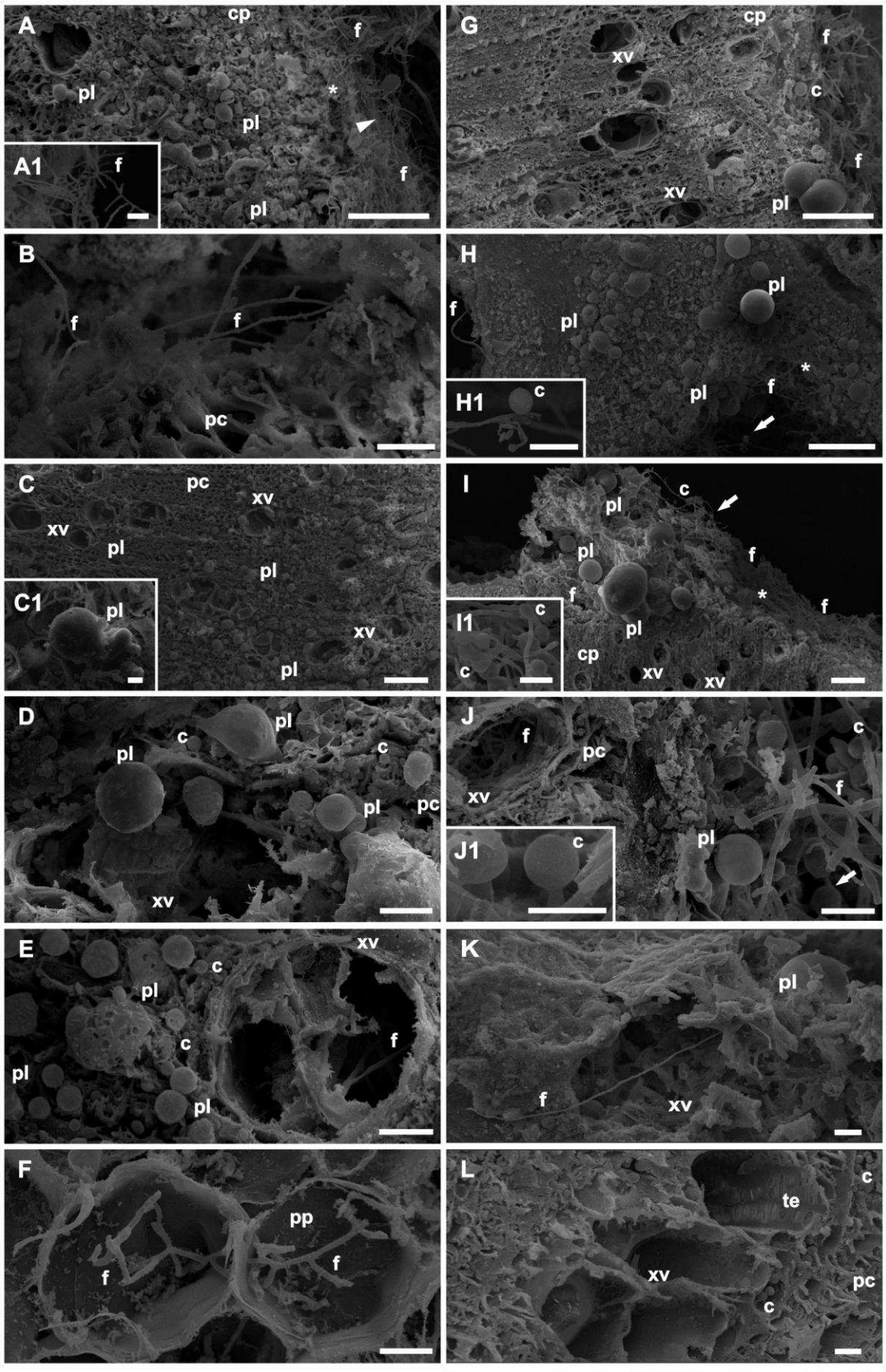
A
cp
f
pl
*
pl
A1
f
f
pl
G
cp
f
xv
c
f
xv
pl
B
f
f
pc
H
pl
f
pl
*
H1
c
pl
f
C
pc
xv
xv
pl
pl
C1
pl
xv
pl
I
c
pl
pl
f
f
*
f
I1
c
pl
c
cp
xv
xv
D
pl
c
pl
c
pl
pc
xv
J
f
pc
c
xv
f
J1
c
pl
E
xv
c
pl
c
f
pl
pl
K
pl
f
xv
F
pp
f
f
L
c
te
xv
pc
c

Fig. 7

Fig. 7. Scanning electron micrographs of transverse (A, B, C, D, E, F, G, H, I, and J) and longitudinal (K and L) sections of stem tissue from the mango cultivars Haden (A, B, C, D, E and F) and Ubá (G, H, I, J, K and L) at 29 days after inoculation with *Ceratocystis fimbriata*. A, A1 and B: Fungal hyphae grew abundantly in the cortical parenchyma and adjacent to the xylem vessels. Many long fungal hyphae (arrowheads) and perithecia-like structures were observed proximal to the stem region where the inoculation ocurred (asterisks). C and C1: Many perithecia-like structures were visible in the parenchyma cells and in the xylem vessels in the radial direction. D and E: Chlamydospores (aleurioconidia) and perithecia-like structures were abundantly visible in the parenchyma cells among the xylem vessels. The fungal hyphae reached the xylem vessels distant from the inoculation point. F: Hyphae of *C. fimbriata* extensively colonized the pit parenchyma. G, H, H1, I, I1, J and J1: Fungal hyphae, perithecia-like structures and chlamydospores formed or in the process of formation (arrow) were visible in the cortical parenchyma and in the xylem vessels proximal to the stem region where the inoculation occurred (asterisks). K and L: Xylem vessels distal to the inoculation point were free of any occlusion, but fungal hyphae were observed in a few xylem vessels. Chlamydospores were found in the parenchyma cells adjacent to the xylem vessels. Chlamydospores (c), cortical parenchyma (cp), fungal hyphae (f), parenchyma cells (pc), perithecia-like structures (pl), pith parenchyma (pp) and xylem vessels (xv). Scale bars in A1, B, C1, D, E, F, H1, I1, J, J1, K and L = 20 µm and in A, C, G, H and I = 100 µm.

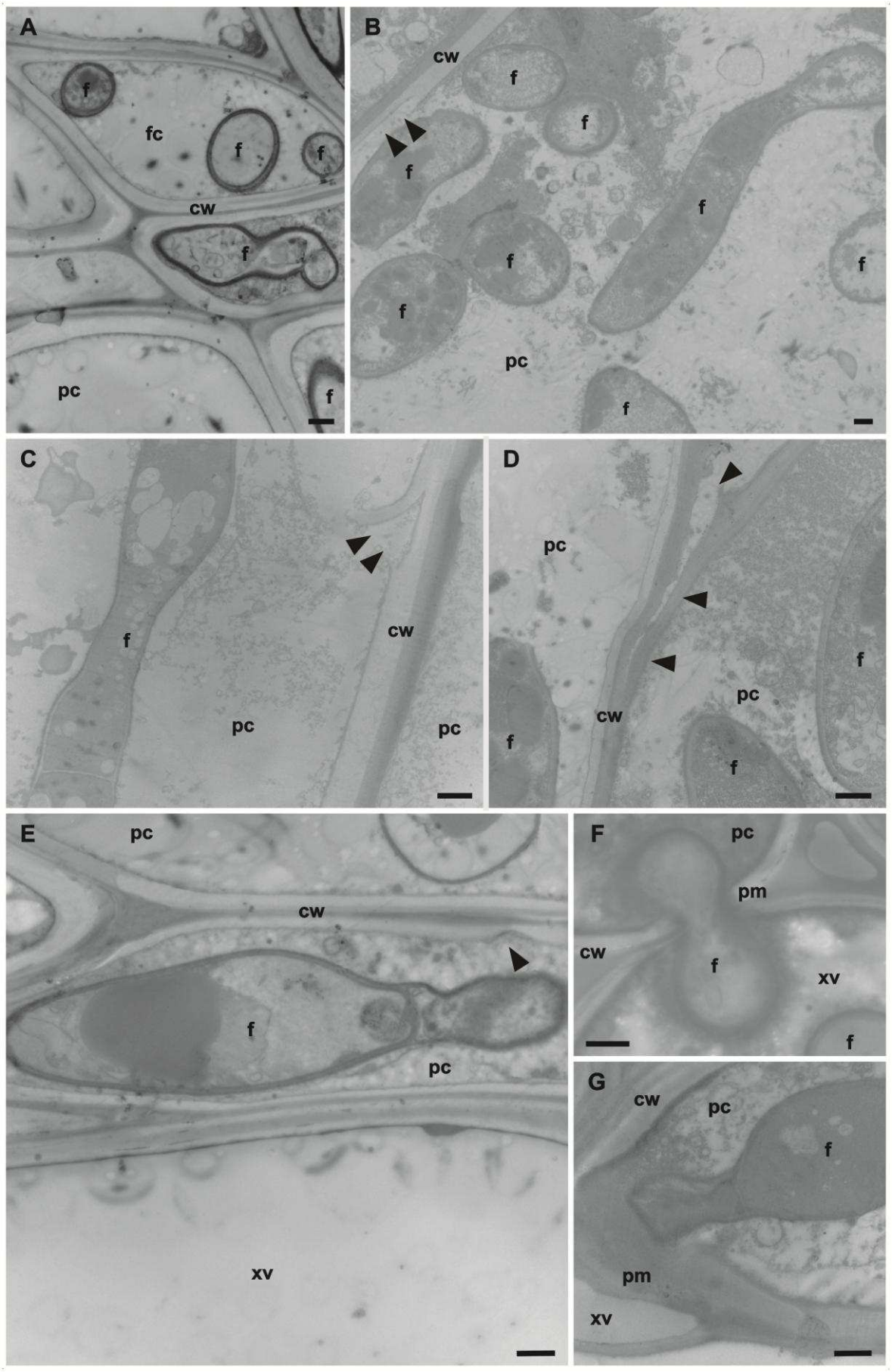
A
f
fc
f
f
cw
f
pc
f
B
cw
f
f
f
f
f
f
f
pc
f
C
f
cw
pc
pc
D
pc
f
pc
cw
f
f
E
pc
cw
f
pc
xv
F
pc
pm
cw
f
xv
f
G
cw
pc
f
pm
xv

Fig. 8

Fig. 8. Transmission electron micrographs of transverse (A, E and F) and longitudinal (B, C, D and G) sections of stem tissue from the mango cv. Haden 22 days after inoculation with *Ceratocystis fimbriata*. A: Fungal hyphae extensively colonized the fiber cells. B, C and D: Long and thick fungal hyphae that broadly invaded the parenchyma cells and caused intense degradation of host cell walls (arrowheads). E: Long and thick fungal hyphae grew in the parenchyma cells adjacent to the xylem vessels, and the cell wall showed signs of degradation (arrowhead). F: Fungal hyphae penetrated the cell wall between the parenchyma cells and the xylem vessels. Note the extreme constriction of the fungal cell wall as the fungus passes through the pit membrane. G: Thickened fungal hyphae adhered to the pit membrane before reaching the xylem vessels. Host cell wall (cw), fiber cells (fc), fungal hyphae (f), parenchyma cells (pc), pit membrane (pm) and xylem vessels (xv). Scale bars = 1 µm.

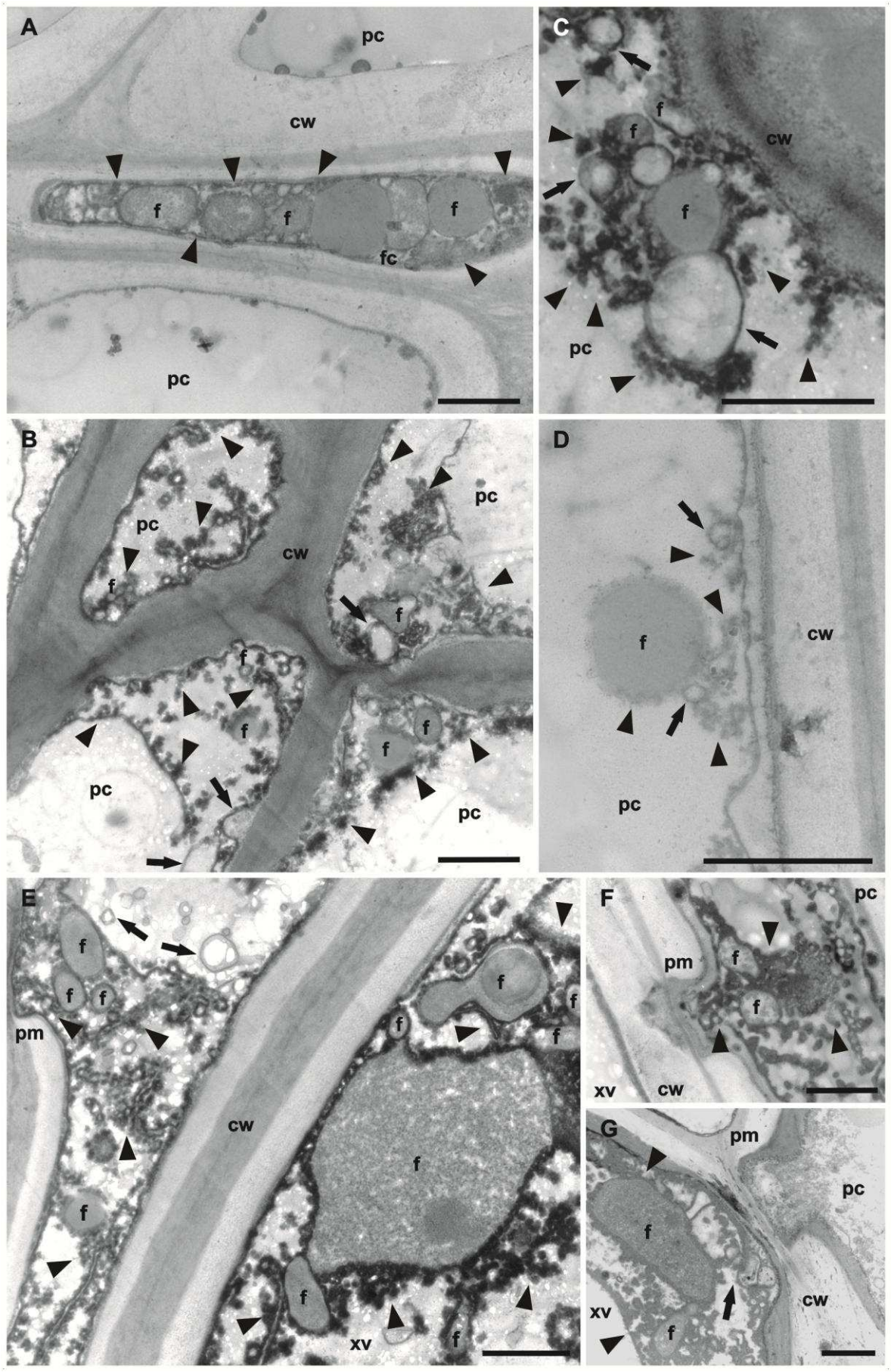
A
pc
cw
f
f
f
fc
pc
C
f
f
cw
f
pc
B
pc
pc
cw
f
f
f
f
f
f
pc
pc
D
f
cw
pc
E
f
f
f
pm
f
f
f
f
cw
f
f
f
xv
F
pc
pm
f
f
xv
cw
G
pm
pc
f
xv
f
cw

Fig. 9

Fig. 9. Transmission electron micrographs of transverse (A, D, F and G) and longitudinal (B, C and E) sections of stem tissue from the mango cv. Ubá 22 days after inoculation with *Ceratocystis fimbriata*. A: Amorphous granular material (arrowheads) accumulated in the fiber cells and regularly interacted with fungal hyphae and the host cell wall. B: Fungal hyphae and the cell wall of the parenchyma cells were surrounded by dense amorphous granular material (arrowheads). Some fungal hyphae appeared dead (arrows). C and D: Fungal hyphae in the parenchyma cells were trapped by the amorphous granular material (arrowheads) and were often killed (arrows). E and F: Fungal hyphae attempting to penetrate the pit membranes were impeded by the amorphous granular material (arrowheads), and several hyphae appeared dead (arrows). G: Fungal hyphae in the xylem vessels were often surrounded by dense amorphous granular material (arrowheads) and several hyphae appeared dead (arrow). Host cell wall (cw), fiber cells (fc), fungal hyphae (f), parenchyma cells (pc), pit membrane (pm) and xylem vessels (xv). Scale bars = 1 µm.

GENERAL CONCLUSIONS

1) The factors mango cultivars and *C. fimbriata* isolates and their interaction were significant for all measures of disease development.

2) Plants from the cultivars Espada, Haden and Palmer inoculated with isolates of *C. fimbriata* were more susceptible, than plants from the cultivars Tommy and Ubá were moderately resistant and resistant, respectively based on the disease progress.

3) Histopathologically, fungal isolates massively colonized the stem tissues of plants of the susceptible cultivars Espada, Haden and Palmer, starting from the collenchyma and moving in the direction of the cortical parenchyma, xylem vessels and pith parenchyma. By contrast, on the stem tissues of plants from the resistant cultivars Tommy Atkins and Ubá, most of the cells reacted to *C. fimbriata* infection by accumulating amorphous material.

4) Tissue proximal to the internal necrotic areas in the stem sections obtained from Ubá had stronger autofluorescence compared to Haden.

5) The peaks and deposition of bound or insoluble S and Ca in the stem tissue from Ubá attacked by *C. fimbriata* were always higher than those produced by tissues of the Haden.

6) SEM observations showed that long fungal hyphae, chlamydospores and perithecia-like structures of *C. fimbriata* were found in abundant in the stem tissue from Haden compared with Ubá.

7) TEM observations showed that long, thickened fungal hyphae in fiber and parenchyma cells as well as in the xylem vessels of the Haden. However, in Ubá hyphae were thin and faint in these same cells and were often surrounded or trapped in dense amorphous granular material, and often hyphae appeared to be dead.

8) The parenchyma cell walls of the Haden colonized by fungal hyphae often showed strong signs of degradation. In contrast, the parenchyma cell walls of Ubá were less degraded and were frequently encrusted by amorphous granular material.

9) Fungal hyphae penetrated the pit membranes of the stem tissue of Haden whereas in tissues of Ubá, fungal penetration was often impeded by amorphous granular material.